J|A|C|S
ARTICLES
Published on Web 11/19/2002

1,2-Dithiin Annelated with Bicyclo[2.2.2]octene Frameworks. One-Electron and Two-Electron Oxidations and Formation of a Novel 2,3,5,6-Tetrathiabicyclo[2.2.2]oct-7-ene Radical Cation with Remarkable Stability Owing to a Strong Transannular Interaction

Atsushi Wakamiya, Tohru Nishinaga, and Koichi Komatsu*

Contribution from the Institute for Chemical Research, Kyoto University, Uji, Kyoto 611-0011, Japan

Received August 27, 2002

Abstract: A stable derivative of 1,2-dithiin annelated with bicyclo[2.2.2]octene frameworks **4** was synthesized as red crystals by the reaction of a dilithiated dimer of bicyclo[2.2.2]octene with elemental sulfur in 59% yield. The cyclic voltammetry of **4** in CH_2Cl_2 at −78 °C showed two reversible oxidation waves at $E_{1/2}$ +0.18 V and +0.72 V versus Fc/Fc^+, indicating that the radical cation and dication of **4** are stable under these conditions. Upon chemical one-electron oxidation of **4** in a rather low concentration (4.0×10^{-4} M) with a 1.5 equiv of $SbCl_5$ in CH_2Cl_2, a radical cation $\mathbf{4}^{\bullet+}$ was formed, whose spin distribution was determined by ESR spectroscopy and by the results of theoretical calculations (UB3LYP/6-31G*). The electronic absorption spectrum of $\mathbf{4}^{\bullet+}$ in CH_2Cl_2 exhibited a maximum absorption at 428 nm ($\epsilon = 2.3 \times 10^3$), which was hypsochromically shifted from that of neutral **4** (469 nm). When the radical cation $\mathbf{4}^{\bullet+}$ was produced in higher concentration (0.06 M) in CH_2Cl_2, a disproportionation was found to take place to give a $SbCl_6^-$ salt of remarkably stable radical cation $\mathbf{5}^{\bullet+}$ having a novel 2,3,5,6-tetrathiabicyclo[2.2.2]oct-7-ene structure. In the X-ray structure of $\mathbf{5}^{\bullet+}SbCl_6^-$, the transannular distance (2.794(3) Å) between the sulfur atoms was found to be less than the sum of the van der Waals radii of a sulfur atom (3.70 Å), suggesting the existence of a bonding interaction between the two disulfide linkages. The theoretical calculations (UB3LYP/6-31G*) suggested that this transannular interaction could be described as the resonance between the limiting structures, each of them having a two-center three-electron bond between two sulfur atoms belonging to two different disulfide linkages: thus, both the spin and positive charge are equally delocalized to the four sulfur atoms, causing a great stabilization of $\mathbf{5}^{\bullet+}$. On the other hand, the 1,2-dithiin radical cation $\mathbf{4}^{\bullet+}$ was found to readily react with triplet oxygen with subsequent rearrangement to give the 1,2-dithiolium derivative $\mathbf{6}^+$ having a carboxyl group. Finally, the reaction of **4** with an excess amount of SbF_5 gave the corresponding dication $\mathbf{4}^{2+}$, which was found to be a 6π aromatic system on the basis of the results of NMR measurement and theoretical calculations.

Introduction

1,2-Dithiins (1,2-dithia-3,5-cyclohexadienes) have attracted considerable interest[1] since the discovery[2] that plants of the sunflower family contain thiarubrine A and B (**1a**,**b**). These 1,2-dithiin derivatives show a wide range of biological activity,[3] probably because of the propensity to readily lose sulfur upon exposure to light or heat to form the corresponding thiophenes **2** (Scheme 1). As concerns their synthesis, the first report on parent 1,2-dithiin **1c** and the 3,6-disubstituted derivatives by

* To whom correspondence should be addressed. Telephone: +81-774-38-3172. Fax: +81-774-38-3178. E-mail: komatsu@scl.kyoto-u.ac.jp.

(1) (a) Viola, H.; Winkler, R. In *HoubenWeyl: Methoden Organische Chemie*; Schaumann, E., Ed.; Thieme: Stuttgart, Germany, 1997; Vol. E9a, pp 209−249. (b) Norton, R. A.; Finlayson, A. J.; Towers, G. H. N. *Phytochemistry* **1985**, *24*, 356−357. (c) Balza, F.; Lopez, I.; Rodriguez, E.; Towers, G. H. N. *Phytochemistry* **1989**, *28*, 3523−3524. (d) Schroth, W.; Dunger, S.; Billig, F.; Spitzner, R.; Herzschuh, R.; Vogt, A.; Jende, T.; Israel, G.; Barche, J.; Ströhl, D. *Tetrahedron* **1996**, *52*, 12677−12698. (e) Huisgen, R.; Kalwinsh, I.; Morán, J. R.; Nöth, H.; Rapp, J. *Liebigs Ann./Recl.* **1997**, 1677−1684. (f) Schroth, W.; Hintzsche, E.; Jordan, H.; Jende, T.; Spitzner, R.; Thondorf, I. *Tetrahedron* **1997**, *53*, 7509−7528. (g) Glass, R. S.; Pollard, J. R.; Schroeder, T. B.; Lichtenberger, D. L.; Block, E.; DeOrazio, R.; Guo, C.; Thiruvazhi, M. *Phosphorus, Sulfur Silicon Relat. Elem.* **1997**, *120/121*, 439−440. (h) Schroth, W.; Spitzner, R.; Bruhn. C. *Eur. J. Org. Chem.* **1998**, 2365−2371. (i) Wang, Y.; Koreeda, M.; Chatterji, T.; Gates, K. S. *J. Org. Chem.* **1998**, *63*, 8644−8645. (j) Block, E. *Phosphorus Sulfur Silicon Relat. Elem.* **1999**, *153/154*, 173−192 and references therein.

(2) (a) Mortensen, J. T.; Sørensen, J. S.; Sørensen, N. A. *Acta Chem. Scand.* **1964**, *18*, 2392−2394. (b) Bohlmann, F.; Kleine, K.-M. *Chem. Ber.* **1965**, *98*, 3081−3086.

(3) (a) Rodriguez, E. In *Biologically Active Natural Products*; Cutler, H. G., Ed.; ACS Symposium Series 380; American Chemical Society: Washington, DC, 1988; pp 432−437. (b) Ellis, S. M.; Balza, F.; Constabel, P.; Hudson, J. B.; Towers, G. H. N. In *Light-Activated Pest Control*; ACS Symposium Series 616; American Chemical Society: Washington, DC, 1995; pp 164−178. (c) Freeman, F.; Aregullin, M.; Rodriguez, E. *Rev. Heteroat. Chem.* **1993**, *9*, 1−19. (d) Bierer, D. E.; Dener, J. M.; Dubenko, L. G.; Gerber, R. E.; Litvak, J.; Peterli, St.; Peterli-Roth, P.; Truong, Th. V.; Mao, G.; Bauer, B. E. *J. Med. Chem.* **1995**, *38*, 2628−2648. (e) Guillet, G.; Philogène, B. J. R.; O′Meara, J.; Durst, T.; Arnason, J. T. *Phytochemistry* **1997**, *46*, 495−498. (f) Page, J. E.; Huffman, M. A.; Smith, V.; Towers, G. H. N. *J. Chem. Ecol.* **1997**, *23*, 2211−2226. (g) De Viala, S. S.; Brodie, B. B.; Rodriguez, E.; Gibson, D. M. *J. Nematol.* **1998**, *30*, 192−200 and references therein.

10.1021/ja028297j CCC: $22.00

Scheme 1

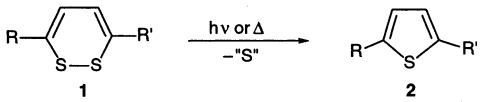

1 **2**

a : R = -C≡CC≡CCH=CH_2, R' = -C≡CMe
b : R = -C≡CCH=CH_2, R' = -C≡CC≡CMe
c : R = R' = H

Schroth et al.[4] appeared soon after the discovery of thiarubrines. However, because of the intrinsic instability of the 1,2-dithiin ring, the synthesis and characterization of other derivatives have been quite limited until recently, when convenient synthetic routes for 1,2-dithiins were developed.[5,6] For example, Koreeda et al.[5a] and Block et al.[5b] independently succeeded in the total synthesis of thiaruburine A and B, respectively, by the use of versatile thiol-protecting groups. 1,2-Dithiins are also interesting molecules from a theoretical viewpoint:[7] they have a twisted conformation that shows a bright reddish-orange color (λ_{max} 410−490 nm)[1a] despite the absence of a normal chromophore. For these reasons, the electronic structure of 1,2-dithiins has been the subject of both studies using theoretical calculations[7a] and those using photoelectron spectroscopy.[7b]

In the chemistry of organosulfur compounds, radical cations play an important role not only as key substances in the creation of functional materials but also as reaction intermediates or as electron-transfer catalysts in organic syntheses and biological redox processes.[8] One of the characteristics of the sulfur radical cation is that two-center three-electron bonds can be formed between the radical cation center and the p-type lone pair electrons of another sulfur atom.[9,10] On the other hand, various cyclic π conjugated systems containing sulfur atom(s) are known in which the spin and positive charge are effectively delocalized on the whole π system, including radical cations and dications.[11] For example, the radical cation salt of thianthrene (dibenzo-1,4-dithiin) is stable enough to be isolated[11d] and can be utilized as a one-electron oxidation reagent.[12] However, cationic 1,4-dithiins without benzo-annelation are not as stable, and neither the isolation of a radical cation salt nor the unambiguous observation of a dication had been reported until our recent studies: we synthesized the 1,4-dithiin annelated with bicyclo-[2.2.2]oct-2-ene (BCO) units, **3**, and succeeded in the first isolation of the stable 1,4-dithiin radical cation salt, $\mathbf{3}^{\bullet+}SbF_6^-$,[13] and the generation of stable dication $\mathbf{3}^{2+}$ as a 6π aromatic species.[14] This remarkable stabilization of cationic species via the annelation with BCO units is ascribed to thermodynamic factors such as inductive and $\sigma-\pi$ conjugative (C−C hyperconjugative) effects,[15,16] as well as kinetic factors such as the steric bulkiness of the bicyclic frameworks and Bredt's rule protection.[16, 17]

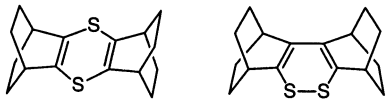

3 **4**

A study concerning 1,2-dithiin synthesis, properties, and chemical and electrochemical oxidation was recently reported.[18] However, the properties of the radical cation and the dication of 1,2-dithiins have not been fully clarified. On the basis of the results of our previous study,[14] it was expected that the 1,2-dithiin bis-annelated with BCO units **4** would yield the radical cation and dication as stable species. Here, we report the full

(4) (a) Schroth, W.; Billing, F.; Reinhold, G. *Angew. Chem., Int. Ed. Engl*. **1967**, *6*, 698−699. (b) Schroth, W.; Billig, F.; Reinhold, G. *Z. Chem*. **1965**, *5*, 352−353. (c) Schroth, W.; Billig, F.; Langoth, H. *Z. Chem*. **1965**, *5*, 353−354.

(5) For example, see: (a) Koreeda, M.; Yang, W. *J. Am. Chem. Soc*. **1994**, *116*, 10793−10794. (b) Block, E.; Guo, C.; Thiruvazhi, M.; Toscano, P. J. *J. Am. Chem. Soc*. **1994**, *116*, 9403−9404. (c) Koreeda, M.; Yang, W. *Synlett* **1994**, 201−203. (d) Koreeda, M.; Wang, Y. *J. Org. Chem*. **1997**, *62*, 446−447. (e) Block, E.; Birringer, M.; He, C. *Angew. Chem., Int. Ed*. **1999**, *38*, 1604−1607.

(6) (a) Schroth, W.; Hintzsche, E.; Spitzner, R.; Irngartinger, H.; Siemund, V. *Tetrahedron Lett*. **1994**, *35*, 1973−1976. (b) Schroth, W.; Hintzsche, E.; Spitzner, R.; Ströhl, D.; Sieler, J. *Tetrahedron*, **1995**, *51*, 13247−13260.

(7) (a) Fabian, J.; Mann, M.; Petiau, M. *J. Mol. Model*. **2000**, *6*, 177−185. (b) Glass, R. S.; Gruhn, N. E.; Lichtenberger, D. L.; Lorance, E.; Pollard, J. R.; Birringer, M.; Block, E.; DeOrazio, R.; He, C.; Shan, Z.; Zhang, X. *J. Am. Chem. Soc*. **2000**, *122*, 5065−5074. (c) Cimiraglia, R.; Fabian, J.; Hess, B. A., Jr. *THEOCHEM* **1991**, *230*, 287−293. (d) Mann, M.; Fabian, J. *THEOCHEM* **1995**, *331*, 51−56. (e) Pitchko, V.; Goddard, J. D. *Chem. Phys. Lett.* **1998**, *289*, 391−395. (f) Ishida, T.; Oe, S.; Aihara, J. *THEOCHEM* **1999**, *461−2*, 553−559. (g) Aihara, J.; Ishida, T. *Bull. Chem. Soc. Jpn*. **1999**, *72*, 937−941. (h) Orlova, G.; Goddard, J. D. *J. Chem. Phys*. **2000**, *112*, 10085−10094.

(8) (a) Glass, R. S. *Top. Curr. Chem*. **1999**, *205*, 1−87. (b) Rusell, G. A.; Law, W. C. In *Sulfur-Centered Reaction Intermediates in Chemistry and Biology*; Chatgilialoglu, C., Asmus, K.-D., Eds.; Plenum Press: New York, 1990; pp 173−183.

(9) (a) Asmus, K.-D. *Acc. Chem. Res*. **1979**, *12*, 436−442. (b) Asmus, K.-D.; Bahnemann, D.; Fischer, Ch.-H.; Veltwisch, D. *J. Am. Chem. Soc*. **1979**, *101*, 5322−5329. (c) Illies, A. J.; Livant, P.; McKee, M. L. *J. Am. Chem. Soc*. **1988**, *110*, 7980−7984. (d) Deng, Y.; Illies, A. J.; James, M. A.; McKee, M. L.; Peschke, M. *J. Am. Chem. Soc*. **1995**, *117*, 420−428. (e) James, M. A.; McKee, M. L.; Illies, A. J. *J. Am. Chem. Soc*. **1996**, *118*, 7836−7842. (f) Maity, D. K. *J. Am. Chem. Soc*. **2002**, *124*, 8321−8328.

(10) In particular, the mesocyclic and acyclic dithioether radical cation and also dication have been extensively studied. For example, see: (a) Musker, W. K. *Acc. Chem. Res*. **1980**, *13*, 200−206. (b) Asmus, K.-D. In *Sulfur-Centered Reaction Intermediates in Chemistry and Biology*; Chatgilialoglu, C., Asmus, K.-D., Eds.; Plenum Press: New York, 1990; pp 155−172. (c) Musker, W. K.; Wolford, T. L. *J. Am. Chem. Soc*. **1976**, *98*, 3055−3056. (d) Musker, W. K.; Roush, P. B. *J. Am. Chem. Soc*. **1976**, *98*, 6745−6746. (e) Doi, J. T.; Musker, W. K. *J. Am. Chem. Soc*. **1978**, *100*, 3533−3536. (f) Musker, W. K.; Wolford, T. L.; Roush, P. B. *J. Am. Chem. Soc*. **1978**, *100*, 6416−6421. (g) Tamaoki, M.; Serita, M.; Shiratori, Y.; Itoh, K. *J. Phys. Chem*. **1989**, *93*, 6052−6058. (h) Iwasaki, F.; Toyoda, N.; Akaishi, R.; Fujihara, H.; Furukawa, N. *Bull. Chem. Soc. Jpn*. **1988**, *61*, 2563−2567. (i) Nenajdenko, V. G.; Shevchenko, N. E.; Balenkova, E. S. *J. Org. Chem*. **1998**, *63*, 2168−2171. (j) Furukawa, N. *Bull. Chem. Soc. Jpn*. **1997**, *70*, 2571−2591 and references therein.

(11) For example, see: (a) Klar, G. In *HoubenWeyl: Methoden Organische Chemie*; Schaumann, E., Ed.; Thieme: Stuttgart, Germany, 1997; Vol. E9a, pp 250−407. (b) Hammerich, O.; Parker, V. D. *Sulfur Rep*. **1981**, *1* (6), 317−396. (c) Duus, F. In *HoubenWeyl: Methoden Organische Chemie*; Schaumann, E., Ed.; Thieme: Stuttgart, Germany, 1993; Vol. E8a, pp 470−629. (d) Bock, H.; Rauschenbach, A.; Näther, C.; Kleine, M.; Havlas, Z. *Chem. Ber*. **1994**, *127*, 2043−2049. (e) Bock, H.; Rauschenbach, A.; Ruppert, K.; Havlas, Z. *Angew. Chem., Int. Ed. Engl*. **1991**, *30*, 714−716.

(12) For example, see: (a) Shine, H. J.; Bae, D. H.; Hoque, A. K. M. M.; Kajstura, A.; Lee, W. K.; Shaw, R. W.; Soroka, M.; Engel, P. S.; Keys, D. E. *Phosphorus Sulfur Relat. Elem.* **1985**, *23* (1−3), 114−142. (b) Lochynski, S.; Shine, H. J.; Soroka, M.; Krishnan, T.; Venkatachalam, T. K. *J. Org. Chem*. **1990**, *55*, 2702−2713. (c) Lochynski, S.; Bogduszek, B.; Shine, H. J. *J. Org. Chem*. **1991**, *56*, 914−920. (d) Chen, T.; Shine, H. J. *J. Org. Chem*. **1996**, *61*, 4716−4719.

(13) Nishinaga, T.; Wakamiya, A.; Komatsu, K. *Tetrahedron Lett*. **1999**, *40*, 4375−4378.

(14) Nishinaga, T.; Wakamiya, A.; Komatsu, K. *Chem. Commun*. **1999**, 777−778.

(15) It is well recognized that hyperconjugative effects are much stronger in cationic species than in neutral molecules because of the decrease in the energy gap between π orbitals and σ orbitals in the cationic state. See: Komatsu, K. *Bull. Chem. Soc. Jpn*. **2001**, *74*, 407−419.

(16) (a) Komatsu, K.; Akamatsu, H.; Jinbu, Y.; Okamoto, K. *J. Am. Chem. Soc*. **1988**, *110*, 633−634. (b) Komatsu, K.; Aonuma, S.; Jinbu, Y.; Tsuji, R.; Hirosawa, C.; Takeuchi, K. *J. Org. Chem*. **1991**, *56*, 195−203. (c) Nishinaga, T.; Komatsu, K.; Sugita, N. *J. Am. Chem. Soc*. **1993**, *115*, 11642−11643. (d) Nishinaga, T.; Komatsu, K.; Sugita, N. *J. Chem. Soc., Chem. Commun*. **1994**, 2319−2320. (e) Komatsu, K. *Eur. J. Org. Chem*. **1999**, 1495−1502. (f) Nishinaga, T.; Izukawa, Y.; Komatasu, K. *J. Am. Chem. Soc*. **2000**, *122*, 9312−9313. (g) Matsuura, A.; Nishinaga, T.; Komatsu, K. *J. Am. Chem. Soc*. **2000**, *122*, 10007−10016. (h) Nishinaga, T.; Inoue, R.; Matsuura, A.; Komatsu, K. *Org. Lett*. **2002**, *4*, 1435−1438.

(17) (a) Gerson, F.; Lopez, J.; Akaba, R.; Nelsen, S. F. *J. Am. Chem. Soc*. **1981**, *103*, 6716−6722. (b) Clark, T.; Teasley, M. F.; Nelsen, S. F.; Wynberg, H. *J. Am. Chem. Soc*. **1987**, *109*, 5719−5724.

(18) Block, E.; Birringer, M.; DeOrazio, R.; Fabian, J.; Glass, R. S.; Guo, C.; He, C.; Lorance, E.; Qian, Q.; Schroeder, T. B.; Shan, Z.; Thiruvazhi, M.; Wilson, G. S.; Zhang, X. *J. Am. Chem. Soc*. **2000**, *122*, 5052−5064.

accounts of the synthesis and one- and two-electron oxidation of **4**, the properties of the obtained radical cation and dication, and the results of the theoretical calculations. In particular, we found that a totally unprecedented disproportionation of the radical cation $\mathbf{4}^{\bullet+}$ takes place to form a unique radical cation having a 2,3,5,6-tetrathiabicyclo[2.2.2]oct-7-ene structure $\mathbf{5}^{\bullet+}$, which exhibits remarkable stability owing to the complete transannular delocalization of spin and charge over the four sulfur atoms. In addition, the radical cation $\mathbf{4}^{\bullet+}$ was found to react with triplet oxygen followed by rearrangement to yield the 6π aromatic 1,2-dithiolium ion derivative $\mathbf{6}^{+}$, whereas the two-electron oxidation of **4** successfully afforded the 6π aromatic 1,2-dithiin dication $\mathbf{4}^{2+}$. The rationalization for these findings based on theoretical calculations will also be described.

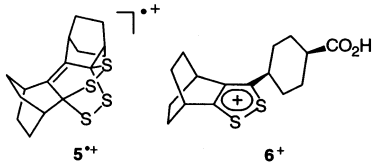

$\mathbf{5}^{\bullet+}$ $\mathbf{6}^{+}$

Result and Discussion

Synthesis of 1,2-Dithiin Annelated with BCO Units, 4. In our previous study,[19] the dilithio derivative of BCO dimer **8** was generated from dibromide **7** by treatment with an excess amount of *tert*-butyllithium in THF at −100 °C, followed by the reaction with elemental sulfur to give thiophene derivative **9** (91%) and a small amount (1−5%) of 1,2-dithiin **4** (Scheme 2). To improve the yield of dithiin **4**, dibromide **7** was converted

Scheme 2 [a]

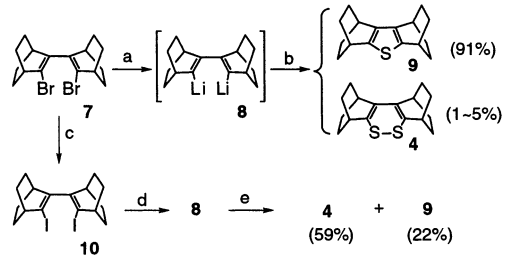

[a] Reagents and conditions: (a) *t*-BuLi (× 15), THF, −100 °C; (b) S_8 (excess) (solid); (c) KI (× 53), CuI (× 20), DMF, 150 °C; (d) *t*-BuLi (× 4), THF, −78 °C; (e) S_n ($n \leq 8$) (× 8) (in toluene).

into diiodide **10** by treatment with an excess amount of KI and CuI in DMF.[20] With diiodide **10,** the dilithiation was found to proceed satisfactorily with 4 equiv of *tert*-butyllithium in THF at −78 °C, and the subsequent treatment with a toluene solution of an excess amount of elemental sulfur gave a much higher yield of 1,2-dithiin **4** (59%) together with thiophene **9** (22%). Here, it was found to be quite important to heat the toluene solution of elemental sulfur to reflux under irradiation of room light for 1 h prior to its addition to the solution of dilithio derivative **8** in order to obtain **4** in a good yield: this treatment of heating and irradiation is considered to convert S_8 into a more reactive form of cyclopolysulfurs with smaller molecular size, S_n ($n < 8$),[21] which is crucial to increase the yield of 1,2-dithiin **4**.

After recrystallization, 1,2-dithiin **4** was obtained as red crystals having an electronic absorption at λ_{max} 463 nm (ϵ 1.9 × 10^2), which is characteristic of 1,2-dithiiins (λ_{max} 410−490 nm).[1a,1d,4a] This 1,2-dithiin **4** was so stable that no apparent decomposition or sulfur extrusion was observed in a CH_2Cl_2 solution under room light and room temperature for at least 6 h, and the crystals could be kept in a freezer (−18 °C) for several months without any decomposition. This remarkable stability is in sharp contrast to the light sensitive nature of other 1,2-dithiin derivatives.[1a,4a,22] The single exception is 1,2-dithiin bis-annelated with 1,7,7-trimethylbicyclo[2.2.1]hept-2-ene (2-bornene) **11**, which showed a similar resistance to sulfur extrusion.[1d,6] Apparently, the common structural feature for **4**

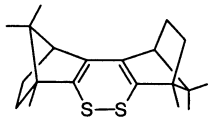

11

and **11** is that $C_\alpha-C_\beta$ bonds in the dithiin ring are rigidly fixed by annelation with bicycloalkene frameworks, which could prevent the rearrangement to the possible intermediate, 2,6-dithiabicyclo[3.1.0]hex-3-ene **12**,[22] in the pathway to the corresponding thiophene by sulfur extrusion (Scheme 3).[1d, 6b]

Scheme 3

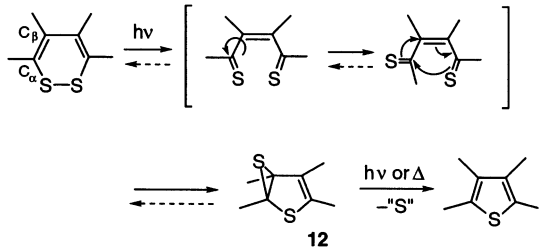

12

Structure of 1,2-Dithiin 4. To compare the structure of 1,2-dithiin **4** with those of the parent compound **1c** and diborneno derivative **11**, the structure of **4** was determined by X-ray crystallography. The geometric parameters determined for the 1,2-dithiin ring in **4** are summarized in Table 1 together with those reported for **1c** (determined in the gas phase by microwave spectroscopy)[23] and **11**.[6a] As shown by the X-ray crystal structure in Figure 1, the dithiin ring of **4** has a typical twisted conformation as reported for other 1,2-dithiins.[1d,23] The C1−S1−S2−C4 dihedral angle of **4** (51.5(2)°) is similar to that of the parent 1,2-dithiin **1c** (53.9°)[23] and larger than that of the diborneno derivative **11** (46.6°).[6a] The bond angles of S1−C1−C2 (122.2(3)°) and C1−C2−C3 (124.3(2)°) of **4** are close to the values of those of the parent 1,2-dithiin **1c** (S1−C1−C2, 121.4°; C1−C2−C3, 124.2°), indicating that the annelation with BCO units does not impose much deformation on the original dithiin ring, while these angles are slightly larger in the diborneno derivative **11** (S1−C1−C2, 123.5°; C1−C2−C3, 125.0°).

Diborneno derivative **11** was reported to have a marked tendency to disproportionate into thiophene **13** and trithiepin **14** (Scheme 4),[1d,6b] probably because of a release of steric

(19) Wakamiya, A.; Nishinaga, T.; Komatsu, K. *Chem. Commun*. **2002**, 1192−1193.
(20) Goldfinger, M. B.; Crawford, K. B.; Swager, T. M. *J. Am. Chem. Soc*. **1997**, *119*, 4578−4593.
(21) Takeda, N.; Tokithoh, N.; Imakubo, T.; Goto, M.; Okazaki, R. *Bull. Chem. Soc. Jpn*. **1995**, *68*, 2757−2764.
(22) Block, E.; Page, J.; Toscano, J. P.; Wang, C.; Zhang, X.; DeOrazio, R.; Guo, C.; Sheridan, R. S.; Towers, G. H. N. *J. Am. Chem. Soc*. **1996**, *118*, 4719−4720.
(23) Gillies, J. Z.; Gillies, C. W.; Cotter, E. A.; Block, E.; DeOrazio, R. *J. Mol. Spectrosc*. **1996**, *180*, 139−144.

Table 1. Geometric Parameters of the Dithiin Ring for **1c**, **11**, **4**, and Cationic Species $\mathbf{4}^{\bullet+}$ and $\mathbf{4}^{2+}$

	1c	11	4		$4^{\bullet+}$	4^{2+}
	exp[a]	exp[b]	exp[c]	calc[d]	calc[e]	calc[f]
			bond length (Å)			
S—S	2.05	2.07	2.0563(19)	2.108	2.106	2.076
S—C	1.76	1.76	1.773(4)	1.785	1.727	1.685
C═C	1.35	1.33	1.337(5)	1.355	1.388	1.444
C—C	1.45	1.44	1.452(7)	1.463	1.434	1.400
			bond angle (deg)			
S—S—C	98.7	99.8	98.81(12)	98.8	105.5	106.6
S—C—C	121.4	123.5	122.2(3)	123.0	129.4	128.8
C—C—C	124.2	125.0	124.3(2)	124.5	125.0	124.6
			torsion angle (deg)			
C—S—S—C	53.9	46.6	51.5(2)	49.8	0.0	0.0
S—S—C—C	-41.2	-36.8	-39.4(3)	-38.8	0.0	0.0
S—C—C—C	0.3	1.8	1.2(6)	0.7	0.0	0.0
C—C—C—C	29	23.7	30.8(8)	27.0	0.0	0.0

[a] Determined in gas phase by microwave spectroscopy (ref 23). [b] Determined by X-ray crystallography (ref 6a). [c] Determined by X-ray crystallography. [d] Calculated at the B3LYP/6-31G* level with a C_2 symmetry constraint. [e] Calculated at the UB3LYP/6-31G* level with a C_{2v} symmetry constraint. [f] Calculated at the B3LYP/6-31G* level with a C_{2v} symmetry constraint.

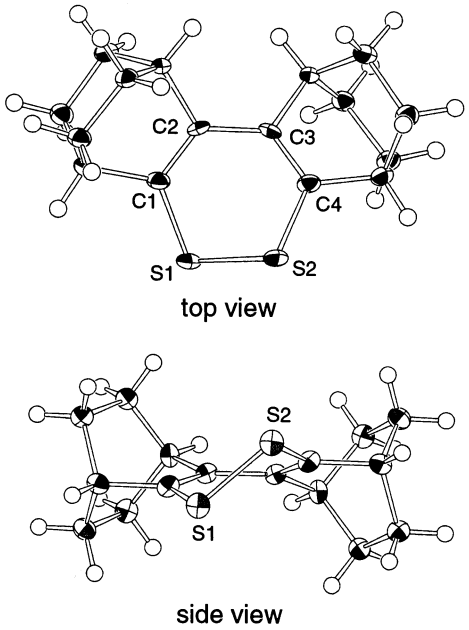

Figure 1. ORTEP drawing of **4**. Thermal ellipsoids are drawn at the 50% probability level.

Scheme 4

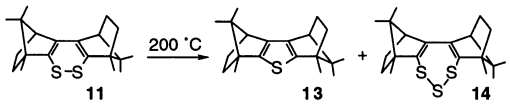

constraint by the rigid 2-bornene units. In contrast, 1,2-dithiin **4** does not undergo such disproportionation, again proving that very little structural strain is imposed by the annelation with BCO units upon the dithiin ring.

Electrochemistry. To examine the redox behavior of **4**, cyclic voltammetry was conducted in CH_2Cl_2 both at room temperature and at −78 °C. As shown in Figure 2, the measurement at room temperature displayed a reversible oxidation wave at $E_{1/2} = +0.18$ V versus Fc/Fc^+,[24] indicating the stability of the radical cation, and an irreversible oxidation wave at $E_{pa} = +0.81$ V (Figure 2a). In comparison with the oxidation potential reported

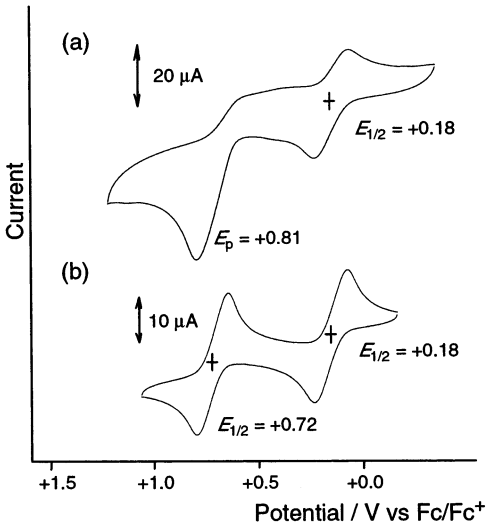

Figure 2. Cyclic voltammograms of **4** in CH_2Cl_2 containing $Bu_4N^+ClO_4^-$ (0.1 M) with a scan rate of 100 mV s^{-1} (a) at room temperature under argon and (b) at −78 °C under vacuum.

Scheme 5

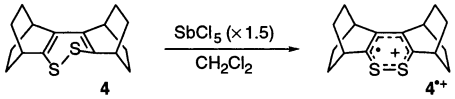

for 3,6-dialkyl-1,2-dithiins[18] ($E_{pa} = +0.46 \sim +0.53$ V vs Fc/Fc^+, calibrated from the potential vs Ag/Ag^+ in CH_3CN[25]), the first oxidation potential of **4** was considerably lowered. This indicates that the HOMO level of **4** was elevated because of the inductive and $\sigma-\pi$ conjugative effects of two bicyclo[2.2.2]-octene (BCO) units. When the cyclic voltammetry was conducted at −78 °C under vacuum, the second oxidation wave turned to a well-defined reversible wave with $E_{1/2} = +0.72$ V (Figure 2b), indicating that not only the radical cation but also the dication of 1,2-dithiin **4** can be stable under these conditions.

Radical Cation of 1,2-Dithiin $\mathbf{4}^{\bullet+}$. (A) ESR Measurement. As the sole example of the generation of the radical cation of a 1,2-dithiin derivative, the one-electron oxidation of 3,6-diphenyl-1,2-dithiin with anhydrous $AlCl_3$ in CH_2Cl_2 has been reported.[18] However, only a broad singlet signal was observed in the ESR spectrum, and no detailed discussion on the spin distribution and chemical reactivity of the radical cation was provided.

The chemical one-electron oxidation of **4** in a rather dilute solution (4.0×10^{-4} M) in CH_2Cl_2 was conducted with 1.5 equiv of $SbCl_5$ under vacuum at room temperature to give a bright yellow solution (Scheme 5) that exhibited a nine-line ESR signal, as shown in Figure 3a. The intensity of this signal did not decrease for at least 2 h at room temperature. To interpret the observed ESR signal and to better understand the electronic structure of the possible radical cation $\mathbf{4}^{\bullet+}$, theoretical calculations (UB3LYP/6-31G*) were carried out. Initially, the opti-

(24) As has been shown, the neutral **4** has a "twisted" conformation, while the radical cation $\mathbf{4}^{\bullet+}$ is considered to be planar, as will be discussed below. Hence, this one-electron oxidation should be considered to proceed through an EC mechanism (ref 18). Although the precise treatment of the electrochemical behavior according to such a mechanism is desirable, as suggested by one referee, we are more interested in a great change in the value of oxidation potential due to the BCO annelation.

(25) $E_{1/2}$(ferrocene) = +0.07 V versus Ag/Ag^+ in CH_3CN. For the calibration of the potential based on the difference in solvent and supporting electrode, see: Connelly, N. G.; Geiger, W. E. *Chem. Rev.* **1996**, *96*, 877−910.

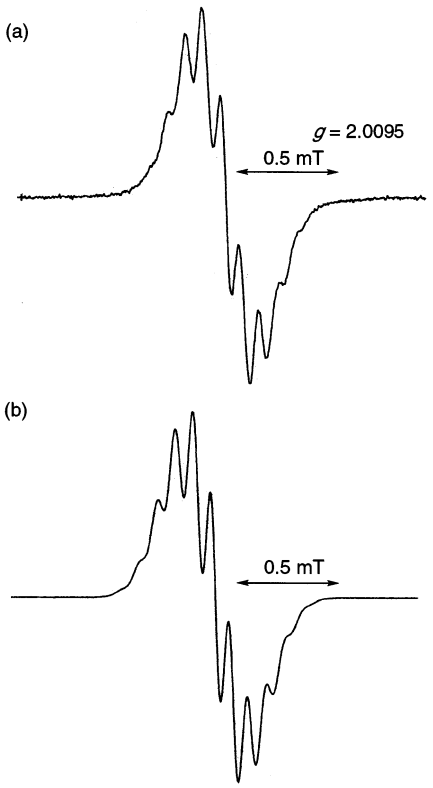

Figure 3. (a) ESR spectrum of $\mathbf{4}^{\bullet+}$ in CH_2Cl_2 at the concentration of 4.0 × 10^{-4} M. (b) Simulation using the calculated ESR coupling constant (B3LYP/6-31G*) at H_α^{anti} (0.073 mT) and H_β^{anti} (0.085 mT) with a line width of 0.075 mT.

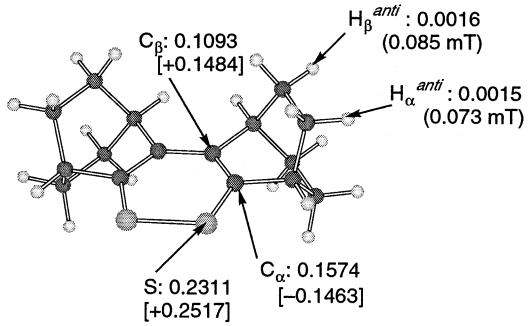

Figure 4. Optimized structure of $\mathbf{4}^{\bullet+}$ at the UB3LYP/6-31G* level, including the selected spin density with the calculated ESR coupling constant shown in round brackets and Mulliken charge shown in square brackets.

mization was made with a C_2 symmetry constraint as in neutral **4**. However, the optimized structure of the radical cation was found to become planar[18] (C−S−S−C dihedral angle = 0.0°) with the molecular symmetry close to C_{2v}: thus, the final optimization was made with a C_{2v} symmetry constraint. The minimum energy for $\mathbf{4}^{\bullet+}$ with a C_{2v} symmetry was confirmed by frequency calculations.

The optimized structure of $\mathbf{4}^{\bullet+}$ with a planar 1,2-dithiin ring is shown in Figure 4 together with selected spin density and Mulliken charge values. The calculated spin densities on the α and β carbons (0.1574 and 0.1093, respectively) are transmitted to the corresponding *anti*-protons (H_α^{anti}, H_β^{anti}) of the ethano bridge through the bonding with a W-like arrangement. Because of the similar values of spin density on H_α^{anti} and H_β^{anti} (0.0015 and 0.0016, respectively), the signal resulting from the two sets of four equivalent *anti*-protons is expected to become a nine-line signal. The signal simulated using the calculated coupling constants is in good agreement with the experimental spectrum, as shown in Figure 3b, thus confirming that the planar radical cation $\mathbf{4}^{\bullet+}$ has actually been generated as a stable species.

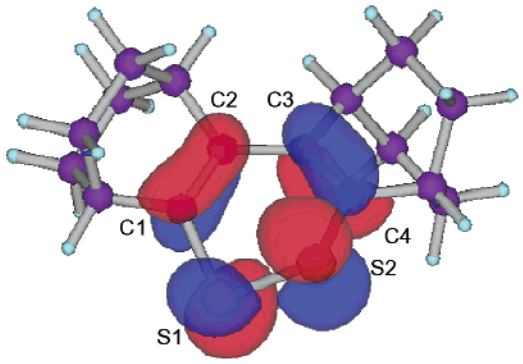

Figure 5. Pictorial presentation of KS HOMO in neutral 1,2-dithiin **4** calculated at the B3LYP/6-31G* level.

(B) Theoretical Calculations. The geometric parameters calculated for the neutral 1,2-dithiin **4** (B3LYP/6-31G*) and radical cation $\mathbf{4}^{\bullet+}$ (UB3LYP/6-31G*) are also included in Table 1. The calculated structural parameters for neutral **4** were in fairly good agreement with the experimental values obtained by X-ray crystallography.

In the optimized structure of radical cation $\mathbf{4}^{\bullet+}$, the lengths of the C1−S1 (1.728 Å) and C2−C3 bonds (1.434 Å) are shortened compared with those of neutral **4** (1.785 and 1.463 Å, respectively), while the length of the C═C bond in $\mathbf{4}^{\bullet+}$ (1.388 Å) is elongated (C═C in **4**, 1.355 Å). The shape of the Kohn−Sham (KS) HOMO of neutral **4** is shown in Figure 5. Upon going from neutral **4** to its radical cation $\mathbf{4}^{\bullet+}$ by removal of one electron from the HOMO, it is reasonable that such bonds as C1−S1 and C2−C3, which are strongly antibonding in the HOMO, are shortened, while the strongly interacting bonds C1−C2 and C3−C4 become elongated. The S−S bond, which has an out-of-phase interaction in the HOMO, should also be shortened, but little difference in the bond lengths is observed upon going from neutral **4** to the radical cation $\mathbf{4}^{\bullet+}$. This may be attributed to the weakened antibonding character of the S−S bond in the HOMO because of the twisted conformation in **4**, which becomes planar in the radical cation $\mathbf{4}^{\bullet+}$.

In comparison with the spin distribution of the radical cation of 1,4-dithiin annelated with the BCO units $\mathbf{3}^{\bullet+}$ (0.2869 on sulfur and 0.1060 on carbon),[13] the spin density on sulfur (0.2311) is smaller and that on α carbons (0.1574) is larger in the 1,2-dithiin radical cation $\mathbf{4}^{\bullet+}$. A unique reactivity of radical cation $\mathbf{4}^{\bullet+}$ derived from this spin distribution will be discussed in detail in a later section.

(C) Electronic Spectrum. In most radical cations, a large bathochromic shift as compared with that of the corresponding neutral species is observed upon one-electron oxidation[26] because of the generally small HOMO−SOMO energy gap. In sharp contrast, the electronic absorption spectrum of $\mathbf{4}^{\bullet+}$ in CH_2Cl_2 exhibited an absorption maximum at 428 nm (2.90 eV), which was hypsochromically shifted from that of neutral **4** (469 nm). Thus, we performed the theoretical calculations (CIS/6-31G*) on **4** and $\mathbf{4}^{\bullet+}$ to interpret this unusual phenomenon.

For the lowest energy transition in a radical cation, two types of transitions are possible, that is, the transition from SOMO

(26) Shida, T.; Iwata, S. *J. Am. Chem. Soc.* **1973**, *95*, 3473−3483.

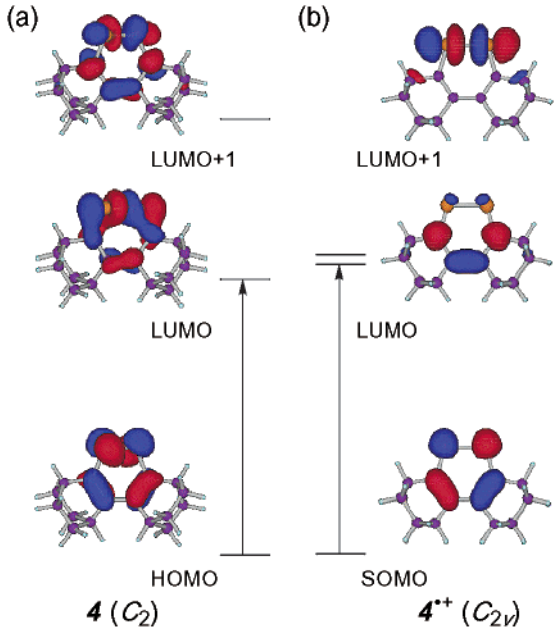

Figure 6. Qualitative MO diagrams of (a) HOMO, LUMO, and LUMO+1 of the 1,2-dithiin **4** (C_2 symmetry) and (b) SOMO, LUMO, and LUMO+1 of the radical cation of 1,2-dithiin **4**$^{\bullet+}$ (C_{2v} symmetry), including a pictorial representation of their molecular orbitals. The SOMO level of **4**$^{\bullet+}$ was placed at the same level as HOMO of **4** for the purpose of comparison.

to LUMO and that from the occupied orbital (HOMO or HOMO-1) to SOMO. In the present case, the absorption at the longest wavelength of **4**$^{\bullet+}$ would correspond to that of the SOMO−LUMO transition because, in the monocyclic, six-membered ring π system of 1,2-dithiin, the difference in energies between occupied orbitals is larger than the SOMO−LUMO energy gap. In fact, the calculated SOMO−LUMO transition energy (2.69 eV) was in fair agreement with the observed value (2.90 eV), while the HOMO−SOMO energy difference was much larger (3.89 eV).

As reported in the previous work,[7a,b] the unusual long wavelength absorption of neutral 1,2-dithiins is interpreted as the transition from the HOMO, which was raised by mixing of the p-type lone pair orbital of two sulfur atoms with the π orbital of the butadiene moiety, to the LUMO, which was lowered by mixing of the σ^* orbital of an S−S bond with the π^* orbital of butadiene, as shown in Figure 6a. As noted previously, upon removal of one electron, the conformation of 1,2-dithiin changes from a twisted structure to a planar one. This affects the molecular orbitals involved in the transition in radical cation **4**$^{\bullet+}$. In the orbitals of **4**$^{\bullet+}$ shown in Figure 6b, the SOMO essentially maintains the π-type coefficients of HOMO in **4** despite the difference in conformation between twisted and planar forms. On the other hand, the σ^* orbital of the S−S bond in **4**$^{\bullet+}$ is destabilized because it can no longer mix with the π^* orbital of the butadiene moiety in the planar conformation.[27] Therefore, the LUMO+1 orbital consists of the σ^* orbital of the S−S bond, while the LUMO in **4**$^{\bullet+}$ consists of the π^* orbital of butadiene. Thus, the transition energy from SOMO to LUMO corresponding to the $\pi-\pi^*$ transition in **4**$^{\bullet+}$ is considered to become larger than that from HOMO to LUMO in **4**, resulting in the hypsochromic shift upon removal of one electron from **4**.

(27) The π^* orbital of butadiene is considered to be stabilized by planarization.

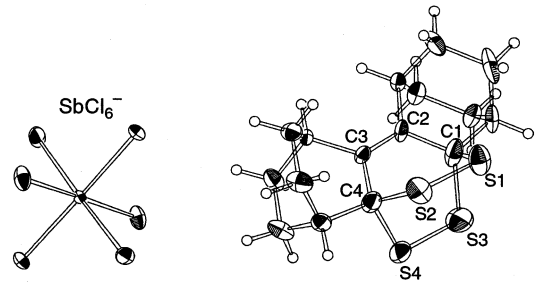

Figure 7. ORTEP drawing of **5**$^{\bullet+}$$SbCl_6^-$. Thermal ellipsoids are drawn at the 30% probability level.

(D) Formation of a Radical Cation Having a 2,3,5,6-Tetrathiabicyclo[2.2.2]oct-7-ene Structure 5$^{\bullet+}$ **from 1,2-Dithiin Radical Cation 4**$^{\bullet+}$. In contrast to the considerable stability of 1,2-dithiin radical cation **4**$^{\bullet+}$ in a CH_2Cl_2 solution with a rather low concentration (4.0×10^{-4} M), an unexpected reaction of **4**$^{\bullet+}$ was found to take place when the concentration was higher. Thus, when the one-electron oxidation of 1,2-dithiin **4** was conducted with $SbCl_5$ (1.5 equiv) in CH_2Cl_2 by the same method as described previously with a concentration of 0.06 M **4**, the initially bright yellow solution changed to a dark green solution within 5 min. Into this solution, hexane was slowly diffused under argon, and orange crystals suited for X-ray crystallography were obtained after the solution was allowed to stand for 7 days. To our surprise, the X-ray crystallographic results for this crystal revealed that it was not the expected radical cation salt **4**$^{\bullet+}$$SbCl_6^-$ but the $SbCl_6^-$ salt of a radical cation having a novel 2,3,5,6-tetrathiabicyclo[2.2.2]oct-7-ene framework, **5**$^{\bullet+}$, as shown in Figure 7. This salt, obtained in 32% yield, was remarkably stable and showed no decomposition upon standing under air for at least one week.

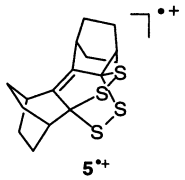

5$^{\bullet+}$

A CH_2Cl_2 solution of this crystal showed a broad single-line ESR signal with $g = 2.010$ at room temperature, supporting the notion that this crystal is a radical cation salt. In the crystal structure of **5**$^{\bullet+}$$SbCl_6^-$, the lengths of the C=C bond and the averaged S−S, C−S, and C(sp^2)−C(sp^3) bond lengths in the central unit were found to be 1.352(8) Å, 1.998(2) Å, 1.850(5) Å, and 1.464(6) Å, respectively (Table 2). The selected bond lengths and angles of both the observed and calculated structures of **5**$^{\bullet+}$ are summarized in Table 2. In particular, it should be noted that the two disulfide linkages are fixed in close proximity to each other. The averaged distance of S1···S3 and S2···S4 was 2.794(3) Å. This value is longer than the typical S−S bond length (2.0 Å) in alkyl disulfide[28] but much shorter than the sum of the van der Waals radii of a sulfur atom (3.70 Å), suggesting the presence of a strong transannular interaction between these sulfur atoms.

The optimized structure of **5**$^{\bullet+}$ calculated at the UB3LYP/6-31G* level (Table 2) reproduced the observed structure fairly well, with the calculated distance of S1···S3 and S2···S4 being

(28) For example, see: Capasso, S.; Zagari, A. *Acta Cryst*. **1981**, *B37*, 1437−1439.

Table 2. Selected Geometric Parameters for $5^{\bullet+}$, 5^{2+}, **5**

	$5^{\bullet+}$		5^{2+}	5
	exp[a]	calc[b]	calc[c]	calc[c]
	bond length (Å)			
S−S	1.998(2)	2.067	2.008	2.130
S−C	1.850(5)	1.889	1.917	1.879
C−C[d]	1.464(6)	1.494	1.476	1.507
C=C	1.352(8)	1.352	1.361	1.348
S···S	2.794(3)	2.923	2.710	3.081
	bond angle (deg)			
S−S−C	103.9(1)	102.2	103.2	101.3
S−C−C[d]	112.4(3)	114.2	117.2	111.5
S−C−S	99.6(3)	101.4	89.9	110.0

[a] Determmined by X-ray crystallography. The values were averaged for C_{2v} symmetry, and esd's of mean values given in parentheses are calculated from the experimental esd's by the following equation: $\sigma(l) = 1/(\Sigma(1/\sigma_i^2))^{1/2}$. [b] Calculated at the UB3LYP/6-31G* level with a C_{2v} symmetry constraint. [c] Calculated at the B3LYP/6-31G* level with a C_{2v} constraint. [d] $C(sp^2)-C(sp^3)$ and $S-C(sp^3)-C(sp^2)$ in the central unit.

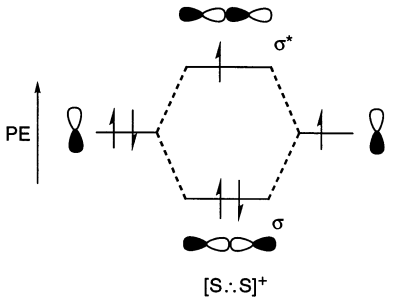

Figure 8. The molecular orbital interaction diagram describing the sulfur p-type lone-pair-based orbitals for a typical 2c-3e S−S bond.

Scheme 6

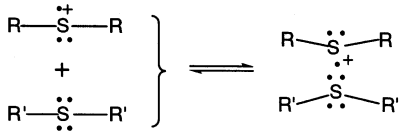

2.923 Å.[29] It was also found that the calculated spin and charge of radical cation $5^{\bullet+}$ were almost exclusively localized on sulfur atoms: the spin and Mulliken charge on each of the four sulfur atoms were 0.229 and +0.258, respectively.

To understand the electronic structure of tetrathiabicyclooctene radical cation $5^{\bullet+}$, it appears pertinent to consider the interactions between the p-type lone pair orbitals on each sulfur atom. In general, the sulfur radical cation tends to form a two-center three-electron (2c-3e) S−S bond intermolecularly with a sulfur atom of another molecule (Scheme 6).[9,30] In an orbital interaction diagram for a typical 2c-3e S−S bond (Figure 8), a p-type orbital on each of the sulfur atoms is arranged for σ-type overlap, resulting in the formation of σ and σ^* molecular orbitals. There are three electrons to be accommodated in these molecular orbitals, resulting in a $2\sigma/1\sigma^*$ electronic ground state with a formal bond order of $^1/_2$.[31] In a similar manner, the

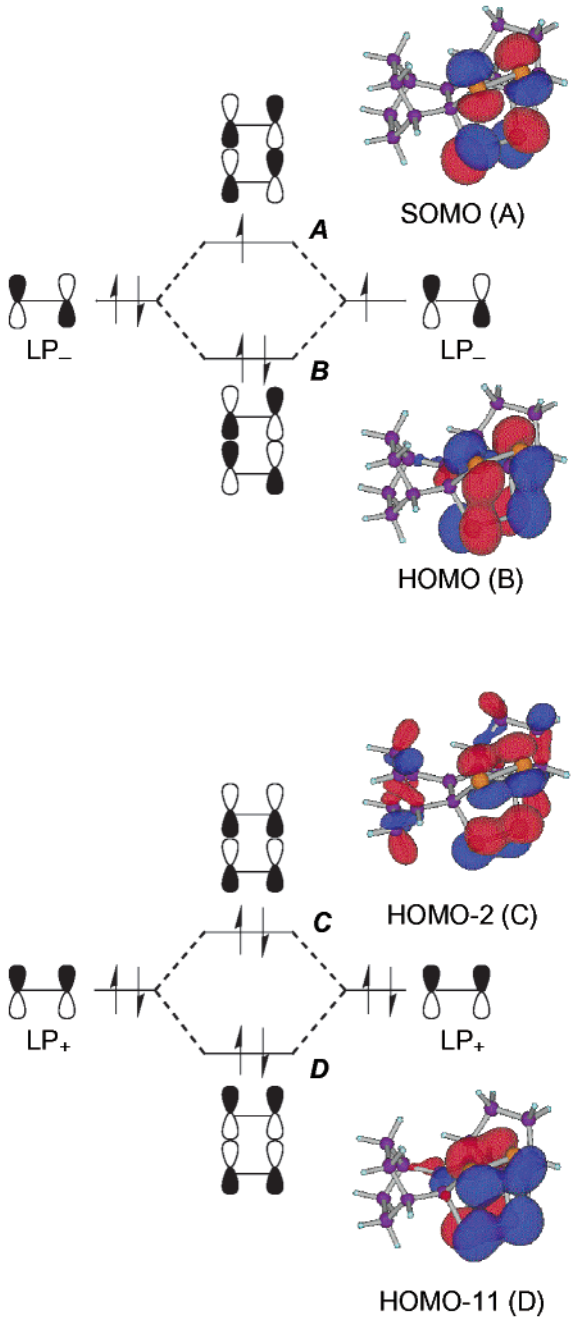

Figure 9. The molecular orbital interaction diagram describing the sulfur p-type lone-pair-based orbitals of disulfides in the radical cation $5^{\bullet+}$, including pictorial representation of SOMO, HOMO, HOMO-2 and HOMO-11 of $5^{\bullet+}$ calculated at the UB3LYP/6-31G* level.

Scheme 7

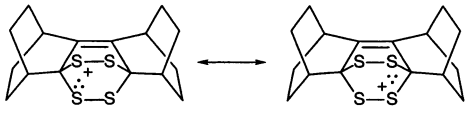

electronic structure of $5^{\bullet+}$ can be described as the resonance hybrid of the limiting structures having a 2c-3e S−S bond, as shown in Scheme 7. Figure 9, in which LP stands for "lone pair", shows the interactions between either the symmetrically (LP_+) or antisymmetrically combined (LP_-) sulfur lone pair orbitals in each of the disulfide units. The two sets of orbitals having proper symmetry interaction ($Lp_- - Lp_-$ and $Lp_+ - Lp_+$) form the four split orbitals of parts A, B, C, and D. In the

(29) The propensity of the slight overestimation of bond length is commonly observed in B3LYP calculations, especially for molecules with third-row elements. See: Ma, B.; Lii, J. H.; Schaefer, H. F., III; Allinger, N. L. *J. Phys. Chem. B* **1996**, *100*, 8763−8769.
(30) (a) Pauling, L. *J. Am. Chem. Soc.* **1931**, *53*, 3225−3237. (b) Clark, T. *J. Am. Chem. Soc.* **1998**, *110*, 1672−1678.
(31) The S−S lone pair−lone pair interaction should depend not only on the distance between sulfur atoms but also on the angle of sulfur−sulfur 3p lone pair orbitals, which was well illustrated by the example of 2,3-dimethyl-5,6-dithiabicyclo[2.1.1]hexane. See: Block, E.; Glass, R. S.; DeOrazio, R.; Lichtenberger, D. L.; Pollard, J. R.; Russell, E. E.; Schroeder, T. B.; Thiruvazhi, M.; Toscano, P. J. *Synlett* **1997**, 525−528.

Scheme 8

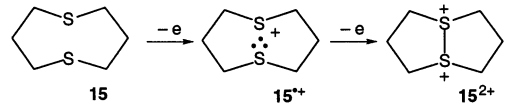

B3LYP calculations, these orbitals appeared in SOMO, HOMO, HOMO-2, and HOMO-11. In each drawing of the molecular orbital with the 0.04 au threshold, there is apparent transannular interaction between the p-type lone pair orbitals of disulfide units for the HOMO (B) and HOMO-11 (D), thus supporting the resonance expression in Scheme 7.

It is known that the species having an inter- or intramolecular 2c-3e S−S bond exhibit an electronic absorption in the range from 400 to 650 nm.[9,32] The electronic absorption of radical cation $\mathbf{5}^{\bullet+}$ observed at λ_{max} 429 nm ($\epsilon = 3.2 \times 10^3$) in CH_2Cl_2 is in agreement with the presence of a bond of this type.

For the species having a 2c-3e bond, a further one-electron oxidation should be possible because the electron to be removed is accommodated in the molecular orbital with an antibonding character (Figure 8). This is exemplified by the oxidation of the radical cation of 1,5-dithiacyclooctane $\mathbf{15}^{\bullet+}$ to the corresponding dication $\mathbf{15}^{2+}$ (Scheme 8).[33] Then a question arises as to whether it would be possible to further oxidize $\mathbf{5}^{\bullet+}$ to the corresponding dication $\mathbf{5}^{2+}$. In addition, one may wonder whether it would be possible to reduce $\mathbf{5}^{\bullet+}$ to its neutral state **5**. We therefore carried out theoretical calculations (B3LYP/6-31G*) on dication $\mathbf{5}^{2+}$ and neutral molecule **5**, and the results are shown in Table 2. As concerns the dication $\mathbf{5}^{2+}$, the singlet state was found to be much more stable than the triplet state, and so, this dication was treated as a singlet. Upon comparison of the optimized structures of **5**, $\mathbf{5}^{\bullet+}$, and $\mathbf{5}^{2+}$, the S···S distance between disulfide units and, accordingly, the C−S−C angle were found to become shorter (**5**, 3.081 Å; $\mathbf{5}^{\bullet+}$, 2.923 Å; $\mathbf{5}^{2+}$, 2.710 Å) and narrower (**5**, 110.0°; $\mathbf{5}^{\bullet+}$, 101.4°; $\mathbf{5}^{2+}$, 89.9°) as compound **5** acquired extra positive charge. In addition, the NICS (2) value,[34,35] that is, the NICS value computed at 2 Å above the center of a rectangle made of the four sulfur atoms, was found to be a large negative value, that is, −20.8 for $\mathbf{5}^{2+}$ and −8.4 for **5**. These results suggest that the 6π homoaromatic ring current could be present in the S_4 ring of $\mathbf{5}^{2+}$ and, thus, that the transannular interaction between the sulfur atoms in $\mathbf{5}^{2+}$ (and also in $\mathbf{5}^{\bullet+}$) could be classified as π bonding rather than σ bonding.

Despite this expected homoaromaticity in $\mathbf{5}^{2+}$, an attempted chemical oxidation of $\mathbf{5}^{\bullet+}SbCl_6^-$ in CD_2Cl_2 at −60 °C by the use of an excess amount of SbF_5 resulted in the quantitative formation of the 1,2-dithiin dication $\mathbf{4}^{2+}$, which was confirmed by NMR spectroscopy (see a later section). On the other hand, an attempt to obtain neutral **5** by the chemical reduction of $\mathbf{5}^{\bullet+}$ in CD_2Cl_2 with 1.2 equiv of $Et_4N^+I^-$ resulted in the formation of thiophene derivative **9** by extrusion of sulfur atoms. These results indicate that the aromatic stabilization of the 1,2-dithiin dication is more favorable than the formation of $\mathbf{5}^{2+}$, and for the reduction of $\mathbf{5}^{\bullet+}$, transannular repulsion between filled p-orbitals of sulfur atoms operates to release the excessive sulfur atoms to construct a thiophene aromatic system.

Scheme 9

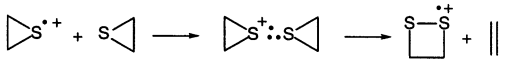

(E) A Possible Mechanism for the Formation of $\mathbf{5}^{\bullet+}$. By detailed examination of the one-electron oxidation of **4** at the higher concentration described previously (0.06 M in CH_2Cl_2), it was found that thiophene **9** (29%), 2-buten-1,4-dione **17** (23%), and the $SbCl_6^-$ salt of a protonated cation of 2-butene-1,4-dione $\mathbf{16}^+$ (2%)[19] were formed in addition to $\mathbf{5}^{\bullet+}SbCl_6^-$ (32%). In our previous study, we found that the radical cation of thiophene annelated with BCO units, $\mathbf{9}^{\bullet+}$, reacts with triplet oxygen in solution to give a protonated cation salt of 2-butene-1,4-dione $\mathbf{16}^+$.[19] This cation $\mathbf{16}^+$ was deprotonated by treatment with water to give **17** quantitatively.[36] Thus, the 2-butene-1,4-dione **17** and its protonated form $\mathbf{16}^+$ are considered to be derived from the thiophene radical cation $\mathbf{9}^{\bullet+}$. Since the neutral 1,2-dithiin derivative **4** is sufficiently stable in CD_2Cl_2 as described previously, the thiophene **9** and its radical cation $\mathbf{9}^{\bullet+}$ must have been derived from the 1,2-dithiin radical cation $\mathbf{4}^{\bullet+}$. The released sulfur atom(s) should be used for the formation of a tetrathiabicyclic framework in $\mathbf{5}^{\bullet+}$. Thus, this can be formally regarded as a disproportionation of the radical cation $\mathbf{4}^{\bullet+}$.

Such sulfur atom migration by way of disproportionation was observed in the reaction of the thiirane radical cation, which involved the 2c-3e S−S bonded dimeric radical cation as a reaction intermediate (Scheme 9).[37] In support of such a bimolecular disproportionation of radical cation $\mathbf{4}^{\bullet+}$, the rate of the reaction was found to be faster when the initial concentration of $\mathbf{4}^{\bullet+}$ in CH_2Cl_2 was higher (5.55×10^{-3} M vs 3.98×10^{-4} M), as determined by UV−vis spectroscopic monitoring (see Supporting Information).

On the basis of the facts mentioned above, one of the possible mechanisms for the formation of $\mathbf{5}^{\bullet+}$ is that shown in Scheme 10. Initially, the radical cation $\mathbf{4}^{\bullet+}$ would intermolecularly react with another radical cation $\mathbf{4}^{\bullet+}$ to give the thiophene radical cation $\mathbf{9}^{\bullet+}$, the neutral thiophene **9**, and the diatomic sulfur radical cation, which could be reduced in situ to form neutral diatomic sulfur.[38] The thiophene radical cation $\mathbf{9}^{\bullet+}$ reacts with oxygen, followed by desulfurization and deprotonation to give 2-butene-1,4-dione **17**, as described previously.[19] Because the spin density in radical cation $\mathbf{4}^{\bullet+}$ is higher on the α carbons (0.1574) than on the β carbons (0.1093), the released diatomic sulfur could be effectively trapped by the radical cation $\mathbf{4}^{\bullet+}$ at α positions to form the radical cation $\mathbf{5}^{\bullet+}$. In support of this mechanism, we found that the isolated yield of $\mathbf{5}^{\bullet+}SbCl_6^-$ increased from 32% to 65% when the reactive sulfur, S_6,[39] was

(32) Chaudhri, S. A.; Mohan, H.; Anklam, E.; Asmus, K.-D. *J. Chem. Soc., Perkin Trans. 2* **1996**, 383−390.
(33) (a) Wilson, G. S.; Swanson, D. D.; Klung, J. T.; Glass, R. S.; Ryan, M. D.; Musker, W. K. *J. Am. Chem. Soc.* **1979**, *101*, 1040−1042. (b) Ryan, M. D.; Swanson, D. D.; Glass, R. S.; Wilson, G. S. *J. Phys. Chem.* **1981**, *85*, 1069−1075. See also ref 10.
(34) For nucleus independent chemical shift (NICS), see: Schleyer, P. v. R.; Maerker, C.; Dransfeld, A.; Jiao, H.; v. Hommes, N. J. R. *J. Am. Chem. Soc.* **1996**, *118*, 6317−6318.
(35) To minimize the effect of local contribution from the p orbital of sulfur atoms, the NICS(2) values were compared for $\mathbf{5}^{2+}$ and **5**. The NICS(0) and NICS(1) values were also calculated: NICS(0), −17.4 ($\mathbf{5}^{2+}$) and −25.8 (**5**); NICS(1), −29.0 ($\mathbf{5}^{2+}$) and −6.4 (**5**). See: Subramanian, G.; Schleyer, P. v. R.; Jiao, H. *Organometallics* **1997**, *16*, 2362−2369.
(36) Wakamiya, A.; Nishinaga, T.; Komatsu, K. Unpublished results. See: Supporting Information.
(37) (a) Qin, X.-Z.; Meng, Q.-C.; Williams, F. *J. Am. Chem. Soc.* **1987**, *109*, 6778−6788. (b) Ekern, S.; Illies, A.; McKee, M. L.; Peschke, M. *J. Am. Chem. Soc.* **1993**, *115*, 12510−12518. (c) Gill, P. M. W.; Weatherall, P.; Radom, L. *J. Am. Chem. Soc.* **1989**, *111*, 2782−2785. (d) Kamata, M.; Murayama, K.; Suzuki, T.; Miyashi, T. *J. Chem. Soc., Chem. Commun.* **1990**, 827−829.

Scheme 10

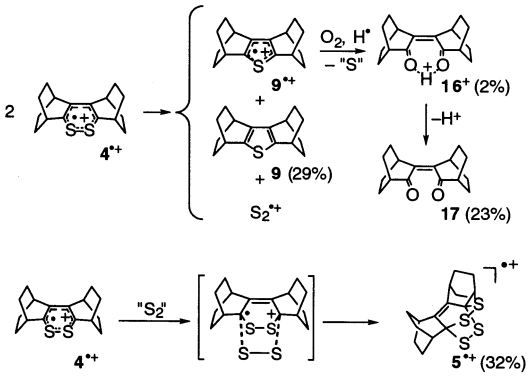

coexistent in the reaction mixture in which the one-electron oxidation of **4** was conducted.

(F) Reaction of 1,2-Dithiin Radical Cation $4^{\bullet+}$ with Triplet Oxygen. In our previous study, we showed that the thiophene radical cation $9^{\bullet+}$ is extremely reactive to triplet oxygen, affording 16^+ after desulfurization,[19] while the 1,4-dithiin radical cation $3^{\bullet+}$ can survive in air.[13] This difference in reactivities is mainly ascribed to the difference in the spin distributions between $9^{\bullet+}$ and $3^{\bullet+}$. In the thiophene radical cation $9^{\bullet+}$, the spin is mostly localized on α carbons (spin density C_α, 0.4631; S, −0.0744), while in the 1,4-dithiin radical cation $3^{\bullet+}$ it is distributed to sulfur atoms to a much higher extent (spin density C_α, 0.1060; S, 0.2869). In the 1,2-dithiin radical cation $4^{\bullet+}$, the spin densities on sulfur, α carbon, and β carbon are calculated to be 0.2311, 0.1574, and 0.1093, respectively, as shown in Figure 4.

Being interested in the effect of this spin distribution on the reactivity of $4^{\bullet+}$, we conducted a reaction of radical cation $4^{\bullet+}$ with triplet oxygen. When radical cation $4^{\bullet+}$ was generated from **4** (24.4 mg) by treatment with 1.5 equiv of $SbCl_5$ in 1.5 mL of $CH_2Cl_2-CH_3CN$ (1:1) and oxygen was introduced into the solution, the ESR measurement indicated that $4^{\bullet+}$ was completely consumed within 1 h. Into this solution, hexane was slowly diffused. After the solution was let stand at room temperature for 7 days, remarkably stable pale yellow single crystals were formed. The X-ray crystallography conducted on this crystal revealed that this product was the $SbCl_6^-$ salt of a 1,2-dithiolium-ion derivative having a carboxyl group, $6^+SbCl_6^-$, as shown in Figure 10.[40] The yield of crystalized $6^+SbCl_6^-$ was 49% (Scheme 11), and its NMR data are given in the Experimental Section.

To obtain some insight into a possible reaction mechanism for the formation of 6^+, the reaction was monitored by ^{1}H NMR spectroscopy. The radical cation $4^{\bullet+}$ was generated in CD_2Cl_2 under vacuum, in a glass tube connected to a vacuum line with an NMR tube as a sidearm, as described previously. After the introduction of oxygen, the NMR tube was sealed and subjected to measurement. As shown in Figure 11, the ^{1}H NMR spectrum of this solution after the reaction time of 2 h exhibited four strong signals at δ 3.79, 3.51, 3.35, and 2.78 ppm for the bridgehead protons of the BCO units together with weak signals for the bridgehead protons of 6^+. The former four signals gradually decreased in intensity with a concomitant increase in those of 6^+,[41] indicating that the former four signals could be ascribed to the reaction intermediate. The ^{13}C NMR spectrum of this reaction intermediate showed three signals for the sp^2 carbons at δ 206.2, 164.0, and 141.3 ppm and one signal for a quaternary sp^3 carbon at δ 72.2 ppm, along with 12 signals for the rest of the sp^3 carbons in the region from δ 22.2 to 46.1 ppm. The appearance of three signals for the sp^2 carbons, two of which were shifted further downfield, seems to suggest that these signals corresponded to the carbons of an allyl cation.

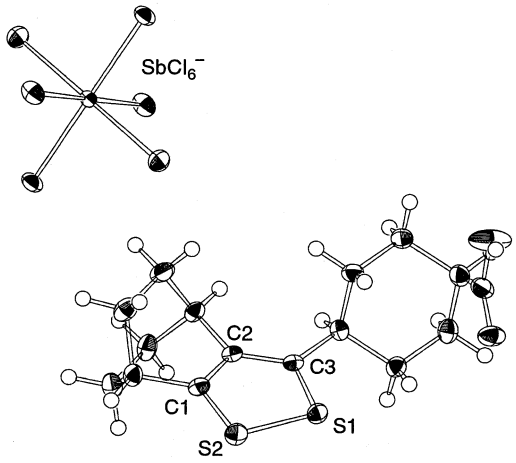

Figure 10. ORTEP drawing of $6^+SbCl_6^-$. Thermal ellipsoids are drawn at the 50% probability level. Selected bond lengths (Å) and angles (deg) are as follows: S1−S2, 2.0205(15); S2−C1, 1.677(4); C1−C2, 1.385(5); C2−C3, 1.386(5); C3−S1, 1.703(4); C3−S1−S2, 96.79(14); S1−S2−C1, 94.68(14); S2−C1−C2, 117.5(3); C1−C2−C3, 116.7(3); C2−C3−S1, 114.3(3).

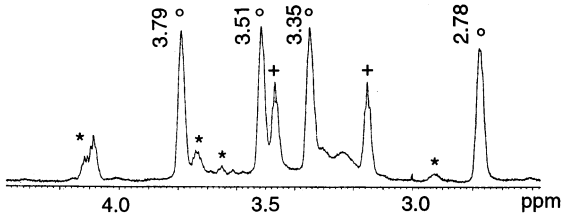

Figure 11. ^{1}H NMR spectrum of the reaction mixture of $4^{\bullet+}$ with oxygen in CD_2Cl_2 after the reaction time of 2 h. The four strong signals marked with ° are supposed to correspond to the reaction intermediate 18^+, while the signals marked with * and + correspond to those for 6^+ and 16^+, respectively. The signals of 18^+ gradually decreased with a concomitant increase in those of 6^+.

Scheme 11

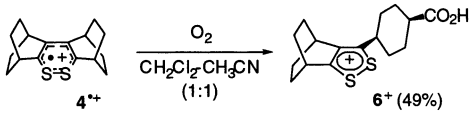

(38) (a) Steliou, K.; Gareau, Y.; Harpp, D. N. *J. Am. Chem. Soc.* **1984**, *106*, 799−801. (b) Steliou, K.; Salama, P.; Brodeur, D.; Gareau, Y. *J. Am. Chem. Soc.* **1987**, *109*, 926−927. (c) Orahovatz, A.; Levinson, M. I.; Carroll, P. J.; Lakshmikantham, M. V.; Cava, M. P. *J. Org. Chem.* **1985**, *50*, 1550−1552. (d) Bartlett, P. D.; Ghosh, T. *J. Org. Chem.* **1987**, *52*, 4937−4943. (e) Ando, W.; Sonobe, H.; Akasaka, T. *Tetrahedron Lett.* **1987**, *28*, 6653−6656. (f) Ando, W.; Kumamoto, Y.; Tokitoh, N. *Tetrahedron Lett.* **1987**, *28*, 4833−4836. (g) Schmidt, M.; Görl, U. *Angew. Chem., Int. Ed. Engl.* **1987**, *26*, 887−888. (h) Nicolaou, K. C.; Hwang, C.-K.; Duggan, M. E.; Carroll, P. J. *J. Am. Chem. Soc.* **1987**, *109*, 3801−3802. (i) Nicolaou, K. C.; Hwang, C.-K.; DeFrees, S.; Stylianides, N. A. *J. Am. Chem. Soc.* **1988**, *110*, 4868−4869. (j) Bender, H.; Carnovale, F.; Peel, J. B,; Wentrup, C. *J. Am. Chem. Soc.* **1988**, *110*, 3458−3461. (k) Harpp, D. N.; MacDonald, J. G. *J. Org. Chem.* **1988**, *53*, 3812−3814. (l) Sato, R.; Satoh, S.; Saito, M. *Chem. Lett.* **1990**, 139−142. (m) Steliou, K.; Gareau, Y.; Milot, G.; Salama, P. *J. Am. Chem. Soc.* **1990**, *112*, 7819−7820.

(39) Mäusle, von H.-J.; Steudel, R. *Z. Anorg. Allg. Chem.* **1980**, *463*, 27−31.

(40) For the typical X-ray structure of the 1,2-dithiolium cation, see for example: Staples, R. J.; Wang, S.; Fackler, J. P., Jr. *Acta Crystallogr.* **1994**, *C50*, 1580−1582. For a review of the 1,2-dithiolium cation, see ref 11c.

(41) In CD_2Cl_2 solution, the conversion from intermediate to product 6^+ was so slow as not to be completed after 48 h. On the other hand, in $CD_2Cl_2-CD_3CN$ (1:1) solution, this conversion was completed within 4 h.

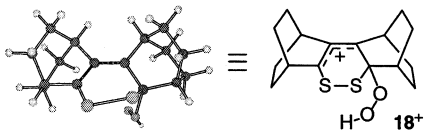

Figure 12. Optimized structure at the B3LYP/6-31G* level as the most possible structure for the reaction intermediate $\mathbf{18}^+$.

Scheme 12

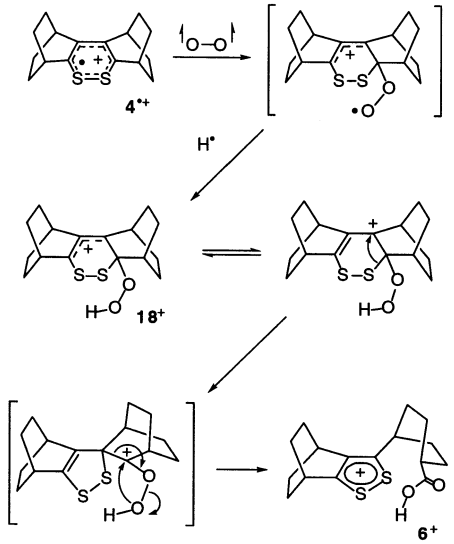

Thus, the most probable structure for this intermediate is thought to be $\mathbf{18}^+$. The theoretical calculations (GIAO/HF/6-31+G**//B3LYP/6-31G*) conducted for $\mathbf{18}^+$ indicated that the expected ^{1}H NMR chemical shifts for the bridgehead protons were δ 3.14, 3.02, 2.89, and 2.23, which were 0.5−0.6 ppm less deshielded than the obtained values. Also, the calculated ^{13}C NMR signals for the allyl cation moiety of $\mathbf{18}^+$ were δ 243.1, 190.0, and 133.6, and that for a quaternary sp^3 carbon was δ 79.4, which could be considered to be roughly in agreement with the observed values. The calculated structure (B3LYP/6-31G*) for $\mathbf{18}^+$ is shown in Figure 12.

On the basis of these results, the possible mechanistic pathway is depicted in Scheme 12. As mentioned previously, the spin density is higher on the α carbon than on the β carbon in the 1,2-dithiin radical cation $\mathbf{4}^{\bullet+}$. Since triplet oxygen readily reacts with an alkene π radical, this reaction is most probably initiated by the addition of triplet oxygen to α carbon. Then, the abstraction of a hydrogen atom either from the solvent or from another molecule of the substrate can give the intermediate $\mathbf{18}^+$.[42] The subsequent 1,2-shift of the S−C bond, followed by the cleavage of a C−C bond of the bicyclo[2.2.2]octane framework and migration of the OH group as shown in Scheme 12, can furnish the final product, 1,2-dithiolium cation $\mathbf{6}^+$.

Dication of 1,2-Dithiin 4. 1,2-Dithiins are cyclic 8π electron systems, and thus, the corresponding dications are expected to benefit from the 6π aromatic stabilization. The cyclic voltammetric results indicated that it is possible to generate the stable dication $\mathbf{4}^{2+}$ by a two-electron oxidation of 1,2-dithiin **4**. Therefore, a chemical two-electron oxidation of **4** with an excess amount of SbF_5 was attempted in CD_2Cl_2 at room temperature in a vacuum-sealed tube. As shown in Table 3, the ^{1}H and ^{13}C NMR spectra of the resulting yellow solution displayed signals at a considerably low field compared with those of the neutral 1,2-dithiin **4**, suggesting the formation of dication $\mathbf{4}^{2+}$ (Scheme 13). The solution of this product was so stable that no decomposition was observed in the vacuum-sealed tube upon standing at −18 °C for several months.

Table 3. ^{1}H and ^{13}C NMR Chemical Shifts for **4** and $\mathbf{4}^{2+}$

compound		δ_H CH	δ_H CH_2	δ_C C=C	δ_C CH	δ_C CH_2
4	obs[a]	2.83[b]	1.62 (8H)	143.1	37.4	27.0
		2.56[c]	1.47 (4H)	126.2	31.9	26.9
			1.35 (4H)			
$\mathbf{4}^{2+}$	obs[a]	4.60[b]	2.52 (8H)	208.2	49.8	25.9
		4.33[c]	2.00 (4H)	160.0	35.3	24.2
			1.82 (4H)			
	calc[d]	4.28[b]	2.91 (*anti*)	253.3	47.8	22.3
		3.81[c]	2.77 (*anti*)	158.5	30.3	20.6
			1.76 (*syn*)			
			1.67 (*syn*)			

[a] In CD_2Cl_2. [b] CH connected to C_α. [c] CH connected to C_β. [d] GIAO/HF/6-31+G*//B3LYP/6-31G*.

Scheme 13

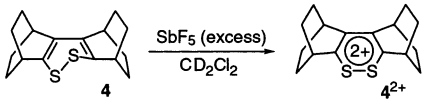

To confirm the generation of the dication $\mathbf{4}^{2+}$ and to better understand its electronic structure, theoretical calculations were conducted to clarify the geometry (B3LYP/6-31G*, Table 1), the NMR chemical shift (GIAO/HF/6-31+G*//B3LYP/6-31G*, Table 3), and the NICS values of dication $\mathbf{4}^{2+}$. Much as in the case for radical cation $\mathbf{4}^{\bullet+}$, the optimized structure of the dithiin ring in $\mathbf{4}^{2+}$ became planar, and thus, the final optimization was made with a C_{2v} symmetry constraint. The ^{1}H and ^{13}C NMR chemical shifts calculated for $\mathbf{4}^{2+}$ were in fair agreement with the observed values, lending support for the formation of dication $\mathbf{4}^{2+}$.

In the observed spectra of $\mathbf{4}^{2+}$, the ^{1}H NMR signals of the bridgehead protons that were located in the same plane as the planar 1,2-dithiin ring exhibited a marked downfield shift of 1.8 ppm as compared with those of neutral **4**. This clearly indicates the presence of a diamagnetic ring current in the dicationic 1,2-dithiin ring and the aromatic character of this 6π electronic system. Furthermore, the NICS value of dication $\mathbf{4}^{2+}$ was calculated to be −6.4, which also supports the aromaticity in this dication. In our previous study,[14] the dication of 1,4-dithiin annelated with BCO units $\mathbf{3}^{2+}$ was prepared in solution and was also found to be a 6π aromatic species. The observed downfield shift of bridgehead protons and the NICS value obtained for dication $\mathbf{4}^{2+}$ are comparable to those of 1,4-dithiin $\mathbf{3}^{2+}$ (2.0 ppm and −8.8, respectively),[14] thus indicating that a similar extent of aromaticity is present in the 1,2-dithiin dication $\mathbf{4}^{2+}$, although it is somewhat smaller than that of 1,4-dithiin dication $\mathbf{3}^{2+}$.

(42) In the reaction of the thiophene radical cation $\mathbf{9}^{\bullet+}$ with oxygen, the thioozonide radical cation $\mathbf{19}^{\bullet+}$ was supposed to be formed. In the case of $\mathbf{4}^{\bullet+}$, the formation of such a C−O−O−C linkage would be difficult due to the relatively long distance between the α carbons in the 1,2-dithiin ring.

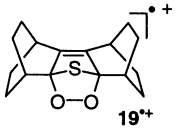

Conclusion

By virtue of the structural modification of the annelation with bicyclo[2.2.2]octene units, the radical cation and dication of 1,2-dithiin have been generated as stable species and their spectral properties have been clarified by the aid of theoretical calculations. In the radical cation $\mathbf{4}^{\bullet+}$, the spin was found to be distributed on the whole 1,2-dithiin π system, and in dication $\mathbf{4}^{2+}$, the presence of 6π aromaticity was demonstrated for the first time. The 1,2-dithiin radical cation $\mathbf{4}^{\bullet+}$ was also found to have a unique reactivity. Under an inert atmosphere, an unusual disproportionation reaction of $\mathbf{4}^{\bullet+}$ took place, producing a novel radical cation having a 2,3,5,6-tetrathiabicyclo[2.2.2]oct-7-ene structure $\mathbf{5}^{\bullet+}$ with remarkable stability despite its rather constrained molecular geometry. This unusual stability was ascribed to a strong transannular interaction between two disulfide linkages, with the spin and the positive charge being evenly distributed among the four sulfur atoms. This structure can be expressed by the resonance structures involving a transannular 2c-3e bond between sulfur atoms. On the other hand, the radical cation $\mathbf{4}^{\bullet+}$ underwent a smooth reaction with triplet oxygen, which was followed by rearrangement to give a 1,2-dithiolium-ion derivative $\mathbf{6}^{+}$. Upon comparison of the results of theoretical calculations, the spin distribution of $\mathbf{4}^{\bullet+}$ was found to be different from that of the thiophene radical cation $\mathbf{9}^{\bullet+}$, in which the spin was mainly localized on α carbons, and also from that of 1,4-dithiin radical cation $\mathbf{3}^{\bullet+}$, in which the spin is localized on sulfur atoms to a larger extent. Thus, it can be concluded that the unique behavior of $\mathbf{4}^{\bullet+}$ can be ascribed to the fairly even spin distribution over the 1,2-dithiin π system and also to the structure of $\mathbf{4}^{\bullet+}$, which can be looked upon as a cisoid butadiene unit with the two ends connected by a reactive disulfide bond.

Experimental Section

General Procedure. ^{1}H (300 MHz) and ^{13}C (75.4 MHz) NMR spectra were recorded on a Varian Mercury-300 spectrometer. Chemical shifts are reported in ppm with reference to tetramethylsilane using the signals of $CHCl_3$, CH_2Cl_2, or CH_3CN as internal standard (δ 7.26, 5.32, and 1.94 in ^{1}H NMR and δ 77.0, 54.0, and 118.7 in ^{13}C NMR, respectively). Mass spectra (EI) were taken on JEOL JMS-HX110 or JMS700 spectrometers. ESR spectra were obtained on a Bruker EMX spectrometer. UV−vis spectra were recorded on a Shimadzu UV-3101-(PC)S spectrometer. Cyclic voltammetry (CV) was performed on a BAS-50W electrochemical analyzer. The CV cell consisted of a glassy carbon working electrode, a Pt wire counter electrode, and a $Ag/AgNO_3$ reference electrode for the measurement at room temperature under argon atmosphere. For the measurement under vacuum at −78 °C, a CV cell consisting of three Pt wires as a working electrode, a counter electrode, and a pseudo-reference electrode was used. The measurements were conducted for the CH_2Cl_2 solutions with the concentration of 1 mM in sample, using tetrabutylammonium perchlorate as a supporting electrolyte (0.1 M); the values for oxidation potentials were calibrated with ferrocene as an internal standard. Preparative gel permeation chromatography (GPC) was performed with a JAI LC-908 chromatograph equipped with JAIGEL 1H and 2H columns.

All experiments were carried out under an argon atmosphere unless otherwise noted. THF and toluene were distilled from sodium benzophenone ketyl. Dichloromethane, acetonitrile, DMF, and hexane were distilled over CaH_2. All the materials were of reagent grade unless otherwise noted.

Computational Method. All calculations were conducted using the Gaussian 98 series of electronic structure programs.[43] The geometries were optimized with the restricted Becke hybrid (B3LYP) method for neutral molecules and singlet dications and with the unrestricted B3LYP (UB3LYP) method for radical cations. The optimization was carried out with proper symmetries, that is, C_2 for **4**, C_{2v} for $\mathbf{4}^{\bullet+}$, C_{2v} for $\mathbf{4}^{2+}$, C_{2v} for **5**, C_{2v} for $\mathbf{5}^{\bullet+}$, and C_{2v} for $\mathbf{5}^{2+}$, and their having minimum energies was confirmed by frequency calculations. The GIAO and NICS calculations were carried out at the HF/6-31+G* level for the optimized geometries at the B3LYP/6-31G* level.

Bis(3-iodobicyclo[2.2.2]oct-2-en-2-yl) (10). A mixture of bis(3-bromobicyclo[2.2.2]oct-2-en-2-yl) (**7**) (0.718 g, 1.91 mmol), KI (17.0 g, 102 mmol), and CuI (7.40 g, 38.0 mmol) in 70 mL of DMF was heated to reflux for 24 h. After the mixture was cooled to room temperature, 10% HCl (30 mL) and ether (50 mL) were added. The organic layer was separated, and the aqueous layer was extracted with ether three times. The combined organic solution was dried over $MgSO_4$, evaporated under reduced pressure, and subjected to flash chromatography over silica gel eluted with hexane−CH_2Cl_2 (1:1) to give almost pure diiodide **10** as a colorless solid. Recrystallization from hexane gave **10** (0.872 g, 98.0%) as colorless crystals: mp 134−136 °C; ^{1}H NMR ($CDCl_3$) δ 2.96 (m, 2H), 2.62 (m, 2H), 1.57 (m, 16H); ^{13}C NMR ($CDCl_3$) δ 152.1, 94.0, 45.8, 37.8, 26.3, 25.9; EI MS *m*/*z* 466 (M^+). HRMS calcd for $C_{16}H_{20}I_2$, 465.9654; found, 465.9662. Anal. Calcd for $C_{16}H_{20}I_2$: C, 41.23; H, 4.32. Found: C, 41.45; H, 4.39.

3,4:5,6-Bis(bicyclo[2.2.2]octeno)-1,2-dithiin (4). To a stirred solution of diiodide **10** (0.296 g, 0.635 mmol) in THF (10 mL) cooled at −78 °C was added *t*-BuLi (1.35 M in pentane, 1.90 mL, 2.67 mmol) dropwise over 2 min. After the mixture was stirred at −78 °C for 20 min, a solution of elemental sulfur (0.208 g, 6.50 mmol) in toluene (5 mL), which had been refluxed under room light for 1 h in advance, was added to the stirred mixture at −78 °C. The reaction mixture was gradually warmed to room temperature over a period of 1 h. After the reaction was quenched with a saturated aqueous solution of NH_4Cl (10 mL), the organic layer was separated, and the aqueous layer was extracted with ether three times. The combined organic solution was dried over $MgSO_4$ and evaporated under reduced pressure to give 0.294 g of a crude product mixture of red and colorless solids which contained 1,2-dithiin **4** and thiophene **9** in about 7:3 molar ratio, as revealed by NMR analysis. Separation of the mixture using preparative GPC eluted with $CHCl_3$ and recrystallization from CH_2Cl_2 layered by CH_3CN afforded 1,2-dithiin **4** (0.104 g, 59%) as red crystals: mp 76−80 °C (dec); UV−vis (CH_2Cl_2) λ_{max} 229 nm (log ϵ 3.48) 270 (3.44), 463 (2.28); ^{1}H NMR ($CDCl_3$) δ 2.83 (m, 2H), 2.58 (m, 2H), 1.59 (m, 8H), 1.50 (m, 4H), 1.37 (m, 4H); ^{13}C NMR ($CDCl_3$) δ 142.4, 125.6, 36.7, 31.3, 26.4, 26.3; EI MS *m*/*z* 276 (M^+). HRMS calcd for $C_{16}H_{20}S_2$, 276.1006; found, 276.0098. Anal. Calcd for $C_{16}H_{20}S_2$: C, 69.51; H, 7.29. Found: C, 69.72; H, 7.40. From the other fraction of GPC separation was obtained **9** (0.0339 g, 22%) as colorless crystals after recrystallization from hexane.[19]

X-ray Crystal Structure Analysis of 4. Single crystals of **4** suitable for X-ray crystal analysis were obtained by slow diffusion of CH_3CN into the CH_2Cl_2 solution of **4** at −18 °C over the period of 3 days. Intensity data were collected at 123 K on a Bruker SMART APEX diffractometer with Mo Kα radiation (λ = 0.71073 Å) and a graphite monochromator. A total of 4481 reflections were measured at a maximum 2θ angle of 50.0°, and 1519 were independent reflections (R_{int} = 0.0266). The structure was solved by direct methods (SHELX-TL) and refined by the full-matrix least-squares on F^2 (SHELEXL-97)

(43) Frisch, M. J.; Trucks, G. W.; Schlegel, H. B.; Scuseria, G. E.; Robb, M. A.; Cheeseman, J. R.; Zakrzewski, V. G.; Montgomery, J. A., Jr.; Stratmann, R. E.; Burant, J. C.; Dapprich, S.; Millam, J. M.; Daniels, A. D.; Kubin, K. N.; Strain, M. C.; Farkas, O.; Tomasi, J.; Barone, V.; Cossi, M.; Cammi, R.; Mennucci, B.; Pomelli, C.; Adamo, C.; Clifford, S.; Ochterski, J.; Petersson, G. A.; Ayala, P. Y.; Cui, Q.; Morokuma, K.; Malick, D. K.; Rabuck, A. D.; Raghavachari, K.; Foresman, J. B.; Cioslowski, J.; Ortiz, J. V.; Stefanov, B. B.; Liu, G.; Liashenko, A.; Piskorz, P.; Komaromi, I.; Gomperts, R.; Martin, R. L.; Fox, D. J.; Keith, T.; Al-Laham, M. A.; Peng, C. Y.; Nanayakkara, A.; Gonzalez, C.; Challacombe, M.; Gill, P. M.; Head-Gordon, M.; Replogle, E. S.; Pople, J. A. *Gaussian 98*, revision A.5; Gaussian, Inc.: Pittsburgh, PA, 1998.

using TWIN instructions. All non-hydrogen atoms were refined anisotropically, and all hydrogen atoms were placed using AFIX instructions. The crystal data are as follows: $C_{16}H_{20}S_2$; FW = 276.44, crystal size 0.40 × 0.40 × 0.40 mm^3, orthorhombic, *C*222(1), a = 7.4957(12) Å, b = 9.8957(15) Å, c = 18.149(3) Å, V = 1346.2(4) Å^3, Z = 4, D_c = 1.364 g cm^{-3}. The refinement converged to R_1 = 0.0518, wR_2 = 0.1417 ($I > 2\sigma(I)$), GOF = 1.223.

Preparation of 1,2-Dithiin Radical Cation 4$^{\bullet+}$. In a ESR tube connected as a sidearm of a Pyrex tube connectable to a vacuum line was placed 1,2-dithiin **4** (1.1 mg, 4.0 × 10^{-3} mmol), while a 1.0 M solution of $SbCl_5$ in CH_2Cl_2 (6 μL, 6 × 10^{-3} mmol) was placed in the Pyrex tube under a stream of argon. The tube was immediately evacuated with cooling by liquid nitrogen. CH_2Cl_2 (10 mL) was dried over CaH_2, degassed by three freeze−pump−thaw cycles, and vapor transferred directly into the cooled tube containing $SbCl_5$. The whole apparatus was sealed under vacuum, and then the solution of $SbCl_5$ in CH_2Cl_2 was poured onto 1,2-dithiin **4** in a ESR tube as a sidearm. The color of the solution immediately turned to bright yellow by mixing. The ESR spectrum was taken on the resulting solution (4.0 × 10^{-4} M) at room temperature to give a nine-line signal (g = 2.0095), as shown in Figure 3.

Exactly in the same way, radical cation **4**$^{\bullet+}$ (4.0 × 10^{-4} M) was generated in CH_2Cl_2 at room temperature under vacuum in a quartz cell (l = 0.10 cm) connected to a sidearm of a Pyrex tube connectable to a vacuum line. The apparatus was sealed under vacuum and subjected to the measurement of a UV−vis spectrum: UV−vis (CH_2Cl_2) λ_{max} 221 nm (log ϵ 4.05) 428 (3.36).

Preparation and Isolation of 5$^{\bullet+}$SbCl$_6^-$. In a sidearm of a Pyrex tube connectable to a vacuum line was placed 1,2-dithiin **4** (24.4 mg, 8.83 × 10^{-2} mmol) while a 1.0 M solution of $SbCl_5$ in CH_2Cl_2 (130 μL, 0.130 mmol) was placed in the Pyrex tube under a stream of argon. The tube was immediately evacuated with cooling by liquid nitrogen. CH_2Cl_2 (1.5 mL) was dried over CaH_2, degassed by three freeze−pump−thaw cycles, and vapor transferred directly into the cooled tube containing $SbCl_5$. Then the connection to the vacuum line was closed, and the Pyrex tube was warmed to room temperature. When **4** was completely dissolved in CH_2Cl_2 containing $SbCl_5$ by mixing, the color of the solution turned to bright yellow, which stayed for about 5 min and then changed into dark green. The tube was connected again to the vacuum line, and the reaction mixture was cooled to −78 °C. Hexane (3.0 mL) was dried over CaH_2, degassed by three freeze−pump−thaw cycles, and vapor transferred and layered directly onto the cooled (−78 °C) solution of **4**$^{\bullet+}$SbCl$_6^-$ in CH_2Cl_2. The tube was refilled with argon. After the solution was kept standing at room temperature for one week, salt **5**$^{\bullet+}$SbCl$_6^-$ (19.1 mg, 32%) was obtained as orange crystals suitable for X-ray analysis by filtration: mp 119−121 °C (dec); UV−vis (CH_2Cl_2) λ_{max} 228 nm (log ϵ 3.94), 274 (4.06), 361 (3.66), 429 (3.62); ESR (1.0 × 10^{-3} M solution in CH_2Cl_2), g = 2.010, a broad singlet signal with a peak-to-peak width 0.16 mT.

The pale yellow crystals of **16**$^+$SbCl$_6^-$ (1.1 mg, 2.0%) were separated from the orange crystals of **5**$^{\bullet+}$SbCl$_6^-$ manually by using tweezers, and the structure was confirmed by X-ray analysis (Supporting Information). The filtrate was washed with water three times, dried over $MgSO_4$, and evaporated under reduced pressure to give 22.2 mg of the crude product, which was found to be a mixture of thiophene **9** and 2-butene-1,4-dione **17** in about 1:1 molar ratio as revealed by NMR analysis. Separation of the mixture by flash chromatography over silica gel eluted with CH_2Cl_2 afforded thiophene **9** (6.2 mg, 29%) as a colorless solid and subsequent elution with ether gave 2-butene-1,4-dione **17** (4.9 mg, 23%) as a pale yellow solid.

In a sidearm of a Pyrex tube connectable to a vacuum line were placed 1,2-dithiin **4** (23.3 mg, 8.43 × 10^{-2} mmol) and S_6[39] (5.40 mg, 1.68 × 10^{-1} mmol), while a 1.0 M solution of $SbCl_5$ in CH_2Cl_2 (126 μL, 0.126 mmol) was placed in the Pyrex tube under a stream of argon. Exactly in the same way as described previously, dried and degassed CH_2Cl_2 (1.5 mL) was vapor transferred into the tube and the reaction mixture including S_6 was dissolved in CH_2Cl_2. When **4** was completely dissolved in CH_2Cl_2 by mixing, the resulting solution took on a dark green coloration. Dried and degassed hexane (3.0 mL) was vapor transferred and layered directly onto the cooled (−78 °C) solution. The tube was refilled with argon. After the solution was kept standing at room temperature for one week, salt **5**$^{\bullet+}$SbCl$_6^-$ (37.2 mg, 65.4%) was obtained as orange crystals by filtration. From the filtrate, thiophene **9** (5.8 mg, 28%) and 2-butene-1,4-dione **17** (1.4 mg, 6.8%) were obtained by the same procedure as described previously.

X-ray Crystal Structure Analysis of 5$^{\bullet+}$SbCl$_6^-$. Intensity data were collected at 123 K on a Bruker SMART APEX diffractometer with Mo Kα radiation (λ = 0.71073 Å) and graphite monochromator. A total of 12811 reflections were measured at a maximum 2θ angle of 50.0°, of which 4015 were independent reflections (R_{int} = 0.0232). The structure was solved by direct methods (SHELXTL) and refined by the full-matrix least-squares on F^2 (SHELEXL-97). All non-hydrogen atoms were refined anisotropically and all hydrogen atoms were placed using AFIX instructions. The crystal data are as follows: $C_{16}H_{20}Cl_6S_4Sb$; FW = 675.01, crystal size 0.40 × 0.35 × 0.35 mm^3, Monochlinic, *P*2(1)/c, a = 8.0506(8) Å, b = 23.896(2) Å, c = 12.1284(11) Å, β = 96.488(2)°, V = 2318.3(4) Å^3, Z = 4, D_c = 1.934 g cm−^{3}. The refinement converged to R_1 = 0.0450, wR_2 = 0.1201 ($I > 2\sigma(I)$), GOF = 1.042.

Chemical Oxidation of Radical Cation of 5$^{\bullet+}$. In an NMR tube connected to a sidearm of a Pyrex tube connectable to a vacuum line was placed salt **5**$^{\bullet+}$SbCl$_6^-$ (22.2 mg, 3.30 × 10^{-2} mmol), while ∼0.1 mL (∼1.4 mmol) of SbF_5 was placed in the Pyrex tube under a stream of argon. The tube was immediately evacuated with cooling by liquid nitrogen. CD_2Cl_2 (0.75 mL) was dried over CaH_2, degassed by three freeze−pump−thaw cycles, and vapor transferred directly into the cooled tube containing SbF_5. The whole apparatus was sealed under vacuum, and a solution of SbF_5 in CD_2Cl_2 was added to salt **5**$^{\bullet+}$SbCl$_6^-$ in an NMR tube at −78 °C. The color of the solution turned from bright yellow to deep yellow by mixing, and then the NMR tube was sealed under vacuum. The ^{1}H and ^{13}C NMR spectra were taken on the resulting solution at −60 °C: ^{1}H NMR (400 MHz, CD_2Cl_2) δ 4.56 (m, 2H), 4.30 (m, 2H), 2.47 (m, 8H), 1.80 (m, 4H), 1.67 (m, 4H); ^{13}C NMR (100 MHz, CD_2Cl_2) δ 207.2, 159.1, 48.7, 34.3, 24.9, 23.2. The ^{1}H and ^{13}C NMR spectra were identical to those of 1,2-dithiin dication **4**$^{2+}$ (see a later section).

Chemical Reduction of Radical Cation of 5$^{\bullet+}$. In an NMR tube connected to a Pyrex tube connectable to a vacuum line were placed salt **5**$^{\bullet+}$SbCl$_6^-$ (20.0 mg, 2.96 × 10^{-2} mmol) and Et$_4$N$^+$I$^-$ (9.49 mg, 3.66 × 10^{-2} mmol). CD_2Cl_2 (0.75 mL) was dried over CaH_2, degassed by three freeze−pump−thaw cycles, and vapor transferred directly into the cooled tube containing salt **5**$^{\bullet+}$SbCl$_6^-$ and Et$_4$N$^+$I$^-$. The NMR tube was sealed under vacuum. When **5**$^{\bullet+}$SbCl$_6^-$ and Et$_4$N$^+$I$^-$ were completely dissolved in CD_2Cl_2 by mixing, the color of the solution turned from bright yellow to pale yellow. The ^{1}H and ^{13}C NMR spectra were taken on the resulting solution at room temperature: ^{1}H NMR (CD_2Cl_2) δ 3.28 (m, 2H), 3.25 (m, 2H), 1.75 (m, 8H), 1.35 (m, 4H), 1.27 (m, 4H); ^{13}C NMR (CD_2Cl_2) δ 140.7, 134.9, 31.8, 30.1, 28.2, 27.6. The ^{1}H and ^{13}C NMR spectra were identical to those of thiophene **9**.[19]

Preparation and Isolation of 6$^+$SbCl$_6^-$. In a Pyrex tube connectable to a vacuum line was dissolved 1,2-dithiin **4** (24.2 mg, 8.75 × 10^{-2} mmol) in 1.5 mL of anhydrous CH_2Cl_2−CH_3CN (1:1), and a 1.0 M solution of $SbCl_5$ in CH_2Cl_2 (130 μL, 0.130 mmol) was added to this solution in the Pyrex tube under a stream of argon. After cooling with liquid nitrogen, the tube was evacuated and refilled with oxygen dried through NaOH at −78 °C. Anhydrous hexane (5 mL) was carefully layered onto the yellow solution of the reaction mixture. After the solution was kept standing at room temperature for one week, salt **6**$^+$SbCl$_6^-$ (27.8 mg, 49.3%) was obtained as pale yellow crystals by filtration: mp 148−150 °C (dec); ^{1}H NMR (CD_3CN) δ 4.04 (m, 1H), 3.70 (m, 1H), 3.62 (m, 1H), 2.80 (m, 1H), 2.22 (m, 2H), 2.07 (m, 4H),

1.97 (m, 2H), 1.79 (m, 4H), 1.42 (q, 4H); ^{13}C NMR (CD_3CN) δ 196.6, 193.2, 176.4, 155.3, 43.2, 39.4, 38.6, 33.6, 31.6, 27.7, 26.2, 25.5. Anal. Calcd for $C_{17}H_{23}Cl_8O_2S_2Sb$: C, 28.01; H, 3.18. Found: C, 28.23; H, 3.25.

X-ray Crystal Structure Analysis of $6^+SbCl_6^-$. Single crystals of $6^+SbCl_6^-$ suitable for X-ray crystal analysis were obtained by slow diffusion of hexane into a solution of $6^+SbCl_6^-$ in $CH_2Cl_2-CH_3CN$ (4:1) over one week. Intensity data were collected at 100 K on a Bruker SMART APEX diffractometer with Mo Kα radiation (λ = 0.71073 Å) and a graphite monochromator. A total of 7893 reflections were measured at a maximum 2θ angle of 55.0°, of which 5077 were independent reflections (R_{int} = 0.0213). The structure was solved by direct methods (SHELXTL) and refined by the full-matrix least-squares on F^2 (SHELEXL-97). All non-hydrogen atoms were refined anisotropically, and all hydrogen atoms were placed using AFIX instructions. The crystal data are as follows: $C_{16}H_{21}Cl_6O_2S_2Sb$; FW = 643.90, crystal size 0.10 × 0.10 × 0.10 mm^3, triclinic, *P*-1, a = 8.0312(6) Å, b = 11.1246(8) Å, c = 14.3052(10) Å, α = 107.7860(10)°, β = 92.8560(10)°, γ = 108.0530(10)°, V = 1142.25(14) Å^3, Z = 2, D_c = 1.872 g cm^{-3}. The refinement converged to R_1 = 0.0385, wR_2 = 0.1035 ($I > 2\sigma(I)$), GOF = 1.066.

NMR Observation of Intermediate 18^+ in the Reaction of $4^{\bullet+}$ with Oxygen. In an NMR tube connected to a Pyrex tube connectable to a vacuum line was placed 1,2-dithiin **4** (16.7 mg, 6.04 × 10^{-2} mmol), while a 1.0 M solution of $SbCl_5$ in CH_2Cl_2 (91 μL, 9.1 × 10^{-2} mmol) was placed in the Pyrex tube under a stream of argon. The tube was immediately evacuated with cooling by liquid nitrogen. CD_2Cl_2 (0.75 mL) was dried over CaH_2, degassed by three freeze−pump−thaw cycles, and vapor transferred directly into the cooled tube containing $SbCl_5$. After closing the connection to the vacuum line, dithiin **4** was mixed with $SbCl_5$ in CH_2Cl_2 at room temperature to generate a bright yellow color of radical cation $4^{\bullet+}$. The connection was immediately opened, and the tube was refilled with oxygen dried through NaOH. After the ESR signal of this solution disappeared (1 h), the tube was evacuated and sealed under vacuum. The ^{1}H and ^{13}C NMR spectra were taken at room temperature. The observed NMR chemical shifts for 18^+: ^{1}H NMR (CD_2Cl_2) δ 3.79 (m, 1H), 3.51 (m, 1H), 3.34 (m, 1H), 2.77 (m, 1H), 2.43−1.46 (m, 16H); ^{13}C NMR (CD_2Cl_2) δ 206.2, 164.0, 141.3, 72.2, 46.1, 38.6, 34.7, 32.9, 31.0, 26.2, 24.8, 24.5, 23.7, 23.5, 22.9, 22.2. Calculated NMR chemical shifts for 18^+ (GIAO/HF/6-31+G**//B3LYP/6-31G*): ^{1}H NMR δ 7.92 (OH), 3.14 (CH), 3.02 (CH), 2.89 (CH), 2.23 (CH), 2.20−1.55 (CH_2). ^{13}C NMR δ 243.1 (allyl cation), 190.0 (allyl cation), 133.6 (allyl cation), 79.4 (S−C−O), 42.3 (CH), 32.8 (CH), 31.7 (CH), 30.3 (CH), 26.0 (CH_2), 23.7 (CH_2), 23.5 (CH_2), 22.4 (CH_2), 22.2 (CH_2), 21.3 (CH_2), 20.8 (CH_2), 19.5 (CH_2).

Preparation of Dication 4^{2+}. In an NMR tube connected to a sidearm of a Pyrex tube connectable to a vacuum line was placed 1,2-dithiin **4** (3.5 mg, 1.3 × 10^{-2} mmol), while ~0.05 mL (~0.7 mmol) of SbF_5 was placed in the Pyrex tube under a stream of argon. The tube was immediately evacuated with cooling by liquid nitrogen. CD_2Cl_2 (0.75 mL) was dried over CaH_2, degassed by three freeze−pump−thaw cycles, and vapor transferred directly into the cooled tube containing SbF_5. The whole apparatus was sealed under vacuum, and a solution of SbF_5 in CD_2Cl_2 was added to **4** in an NMR tube. The color of the solution immediately turned to deep yellow after mixing, and then the NMR tube was sealed under vacuum. The ^{1}H and ^{13}C NMR spectra were taken on the resulting solution at room temperature to give the results shown in Table 3.

Acknowledgment. We thank Professor Ralf Steudel of Technische Universität Berlin and Professor Norihiro Tokitoh and Dr. Takahiro Sasamori of Kyoto University for their valuable advice and fruitful discussions. This work was supported by the Grant-in-Aid for COE Research on Elements Science (No. 12CE2005) from the Ministry of Education, Culture, Sports, Science and Technology, Japan. A.W. thanks JSPS for a Research Fellowship for Young Scientists.

Supporting Information Available: Reaction rate for the transformation of $4^{\bullet+}$ to $5^{\bullet+}$ in different concentrations; deprotonation of 16^+; X-ray structures of **10** and $16^+SbCl_6^-$; ^{1}H and ^{13}C NMR spectra of **4**, 4^{2+}, 6^+, and 18^+; ESR spectrum and UV−vis spectrum of $5^{\bullet+}$; optimized molecular coordinates of **4**, $4^{\bullet+}$, 4^{2+}, $5^{\bullet+}$, 5^{2+}, **5**, and 18^+ at the B3LYP/6-31G* level (PDF). X-ray crystallographic files of **4**, $5^{\bullet+}SbCl_6^-$, $6^+SbCl_6^-$, **10**, and $16^+SbCl_6^-$ (CIF). This material is available free of charge via the Internet at http://pubs.acs.org.

JA028297J